

Aérosols et Pandémies: les exemples de la grippe et de la COVID-19

Raymond Tellier MD MSc FRCPC CSPQ FCCM D(ABMM)
Associate Professor
Dept of Medicine
McGill University

Modes de transmission des virus respiratoires

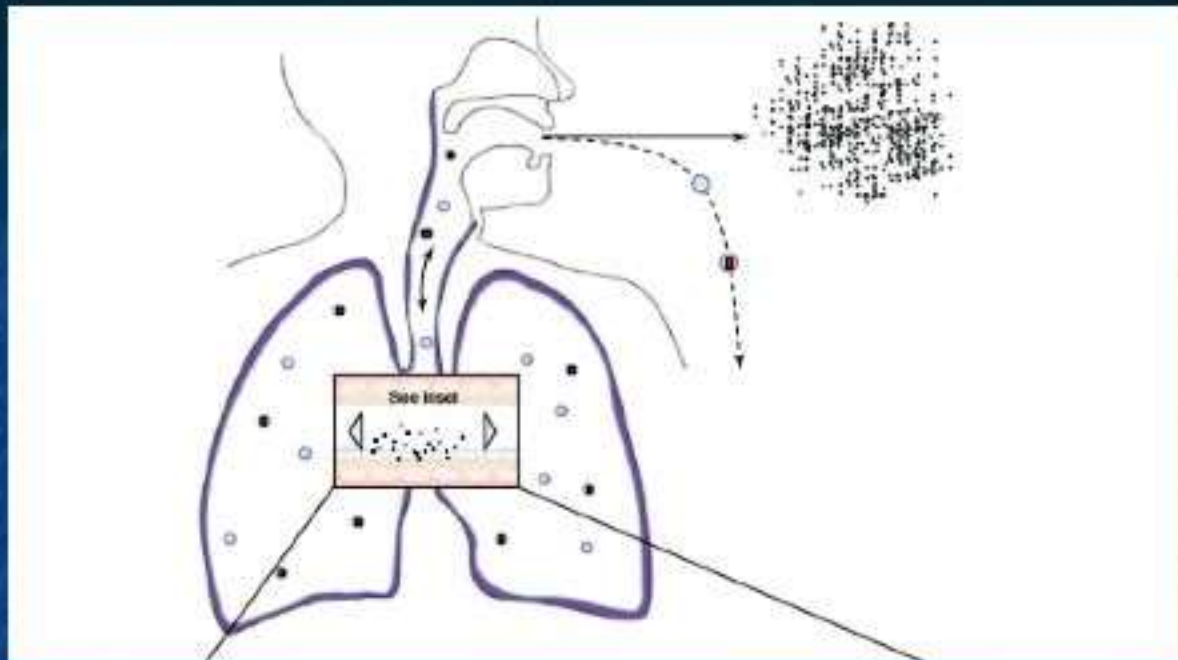
- Aérosols (transmission aérienne [“airborne”])
- Grosses gouttelettes ($> 100 \mu\text{m}$)
- Auto-inoculation via mains contaminées par contacts directs ou indirects (fomites)

Aérosols

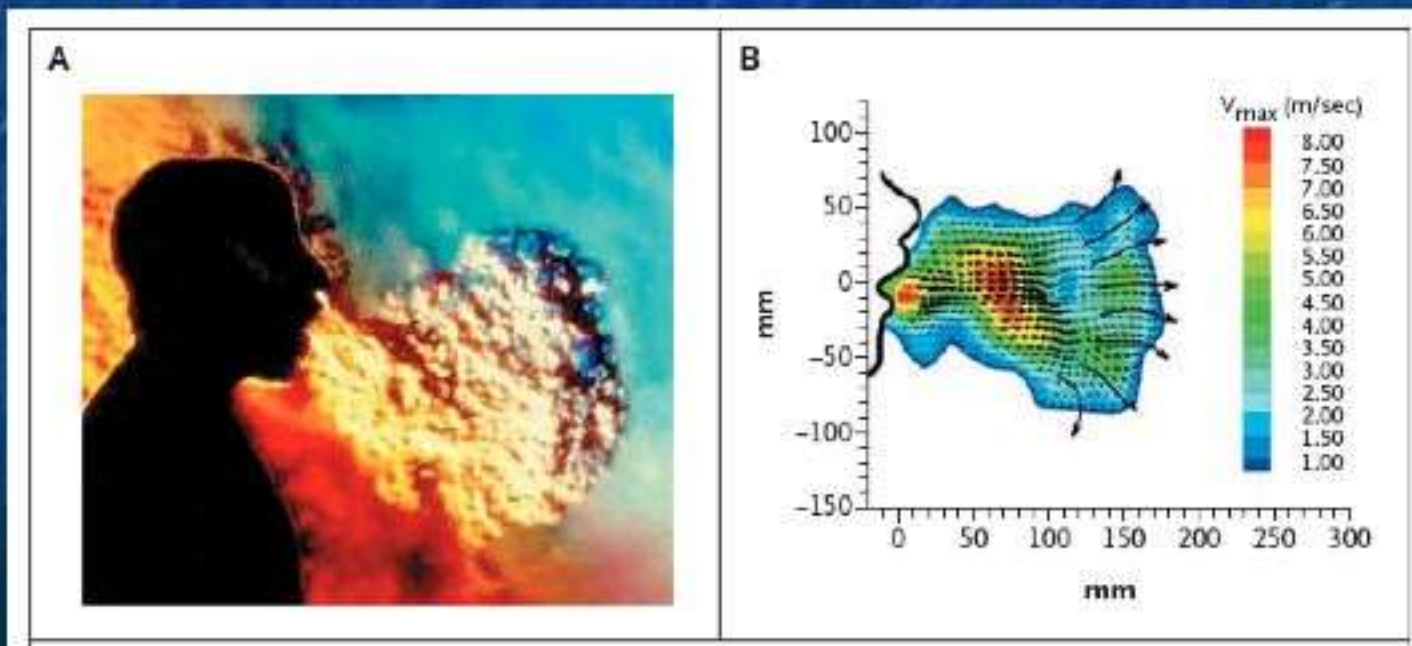
- Les aérosols sont des particules dispersées dans un gaz , suffisamment petites pour rester en suspension pour une longue durée à cause de leur faible vitesse de sédimentation.

Diamètre aérodynamique	Temps de sédimentation, 3m (air sans turbulence)
100 μm	10 sec
40 μm	1 min
20 μm	4 min
10 μm	17 min
5 μm	67 min
3 μm	3.1 hours
1 μm	27.8 hours

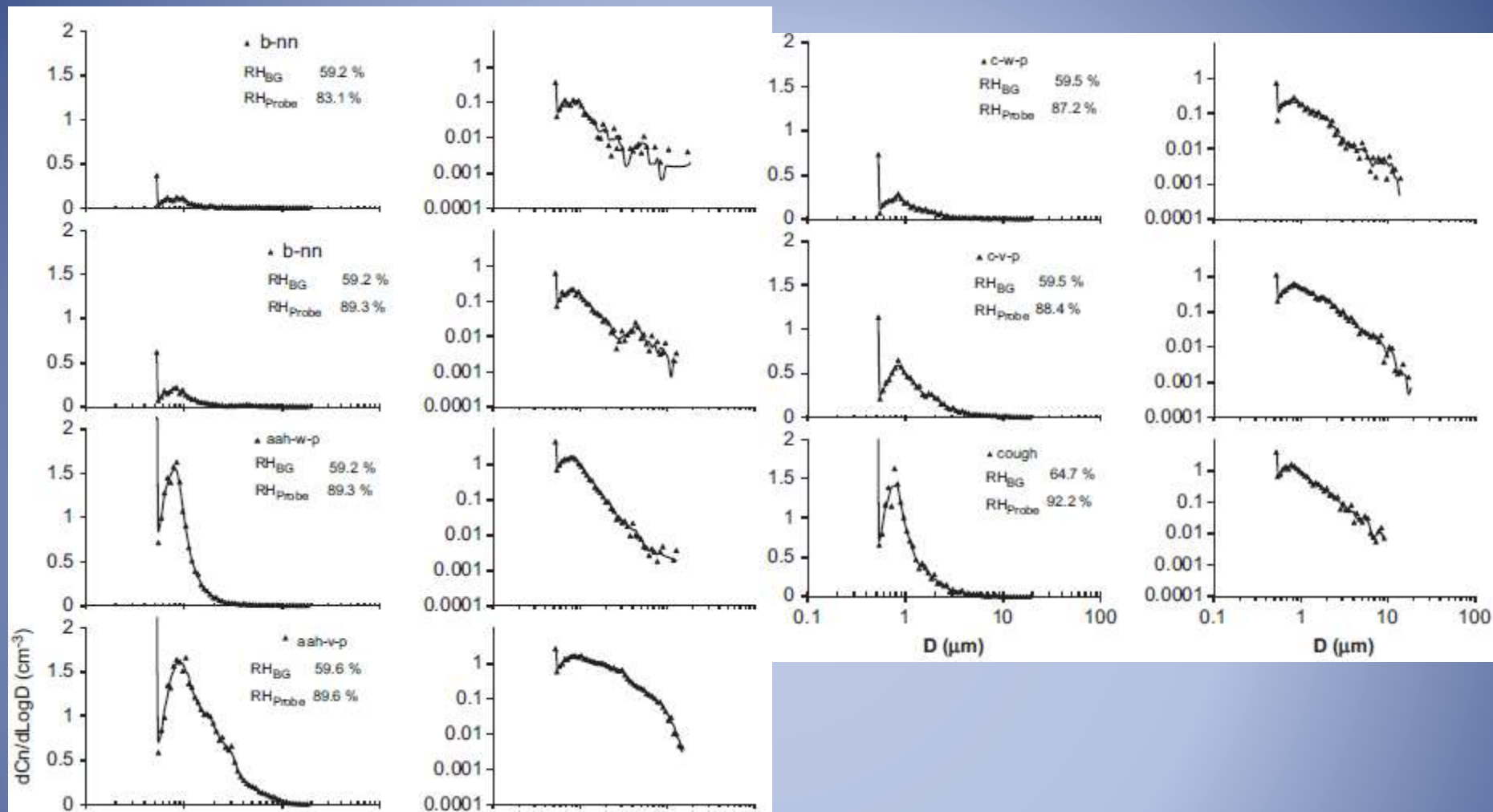
Temps dans le vide:
0.78 sec



Flegel et al,
Drug Discovery Today
2006; 1: 51-57

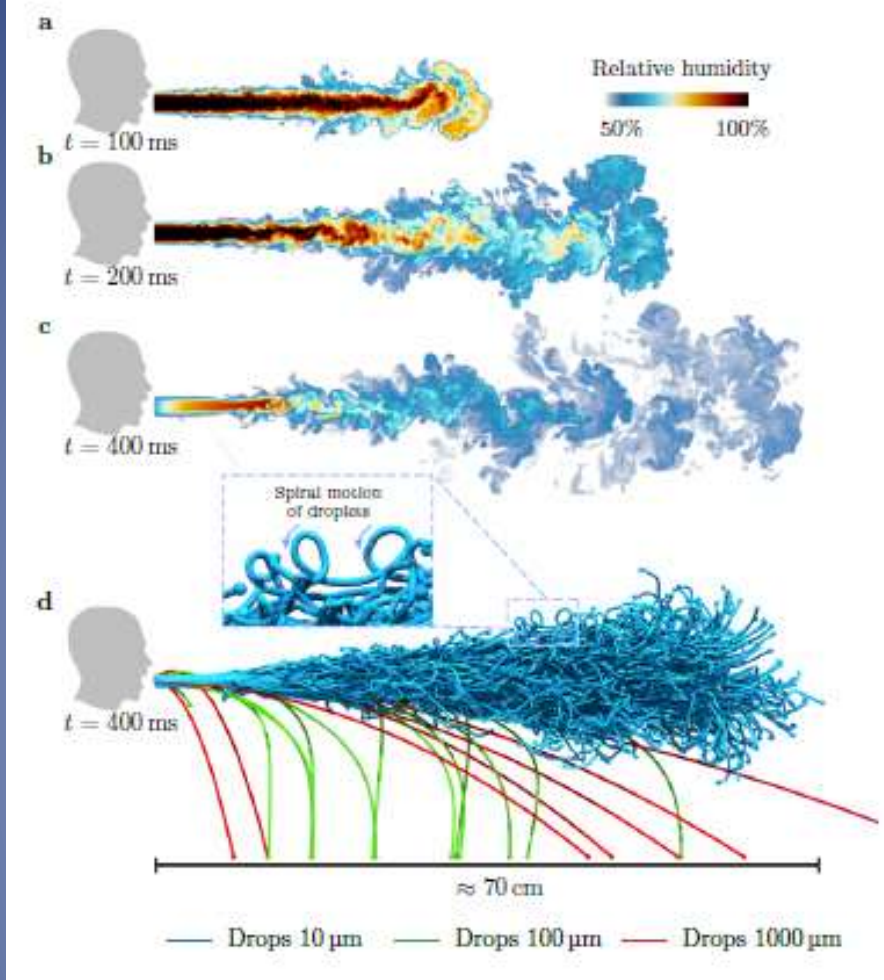


Tang JW, Settles GS
New Engl J Med 2008;
35(:15, e19



Size distribution and sites of origin of droplets expelled from the human respiratory tract during expiratory activities

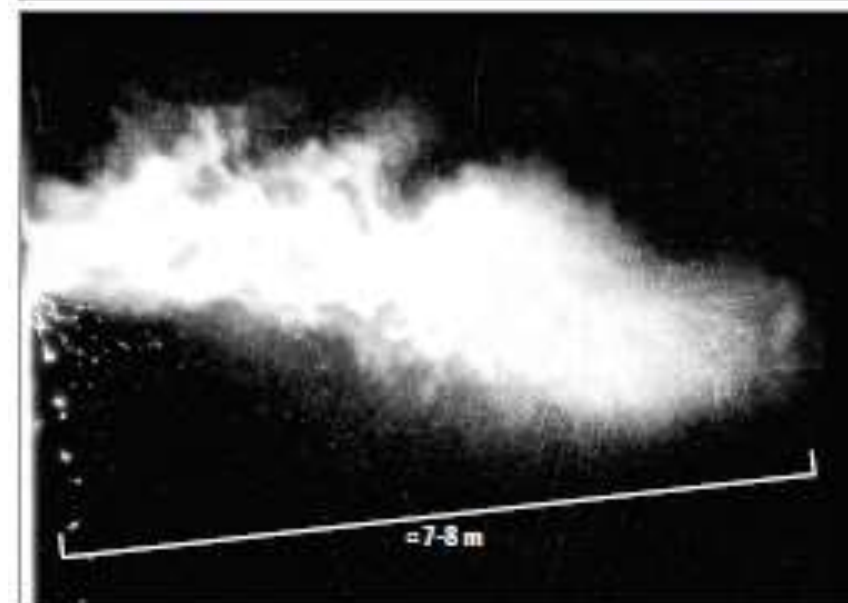
L. Morawska^{a,*}, G.R. Johnson^a, Z.D. Ristovski^a, M. Hargreaves^a, K. Mengersen^a, S. Corbett^b, C.Y.H. Chao^c, Y. Li^d, D. Katoshevski^e



Cheong KL et al Extended lifetime of respiratory droplets in a turbulent vapour puff and its implication on airborne disease transmission Preprint August 2020

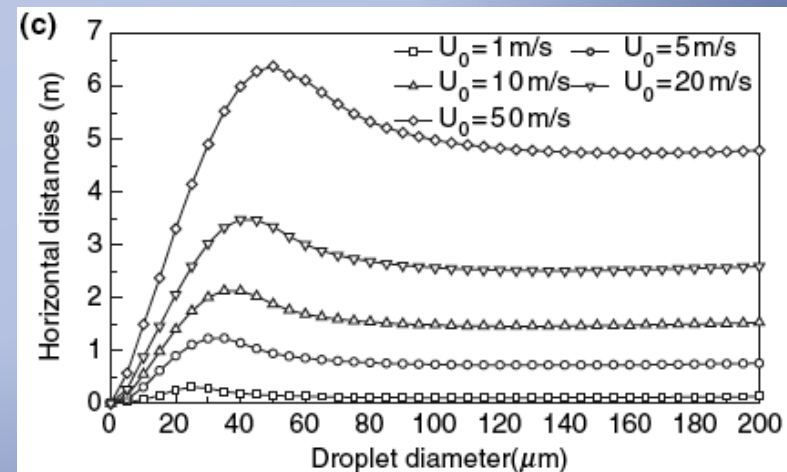
Horizontal distance traveled on an horizontal jet emitted at height of 2m; RH 50% (NaCl 0.9%)
Xie et al Indoor Air 2007; 17: 211-225

Figure. Multiphase Turbulent Gas Cloud From a Human Sneeze



JAMA Insights

Turbulent Gas Clouds and Respiratory Pathogen Emissions Potential Implications for Reducing Transmission of COVID-19
Lydia Bourouiba, PhD



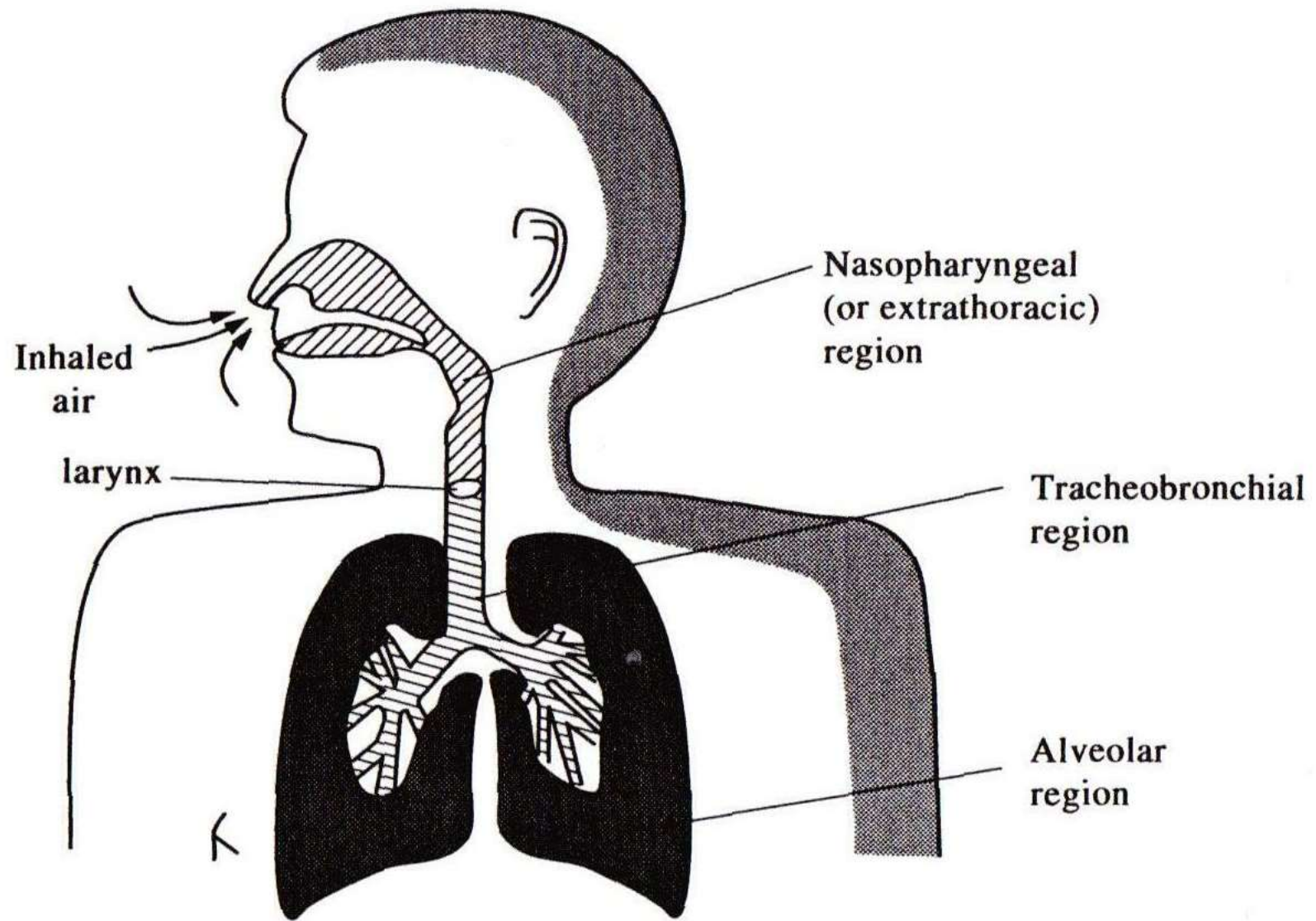


TABLE 11.5 Inhalable, Thoracic, and Respirable Fractions^a

Aerodynamic Diameter (μm)	Inhalable Fraction	Thoracic Fraction	Respirable Fraction
0	1.00	1.00	1.00
1	0.97	0.97	0.97
2	0.94	0.94	0.91
3	0.92	0.92	0.74
4	0.89	0.89	0.50
5	0.87	0.85	0.30
6	0.85	0.81	0.17
8	0.81	0.67	0.05
10	0.77	0.50	0.01
15	0.70	0.19	0.00
20	0.65	0.06	0.00
25	0.61	0.02	0.00
30	0.58	0.01	0.00
35	0.56	0.00	0.00
40	0.55	0.00	0.00
50	0.52	0.00	0.00
60	0.51	0.00	0.00
80	0.50	0.00	0.00
100	0.50	0.00	0.00

^aACGIH (1997).

Hinds WC
Aerosol Technology 2nd ed
John Wiley & Sons
New York 1999

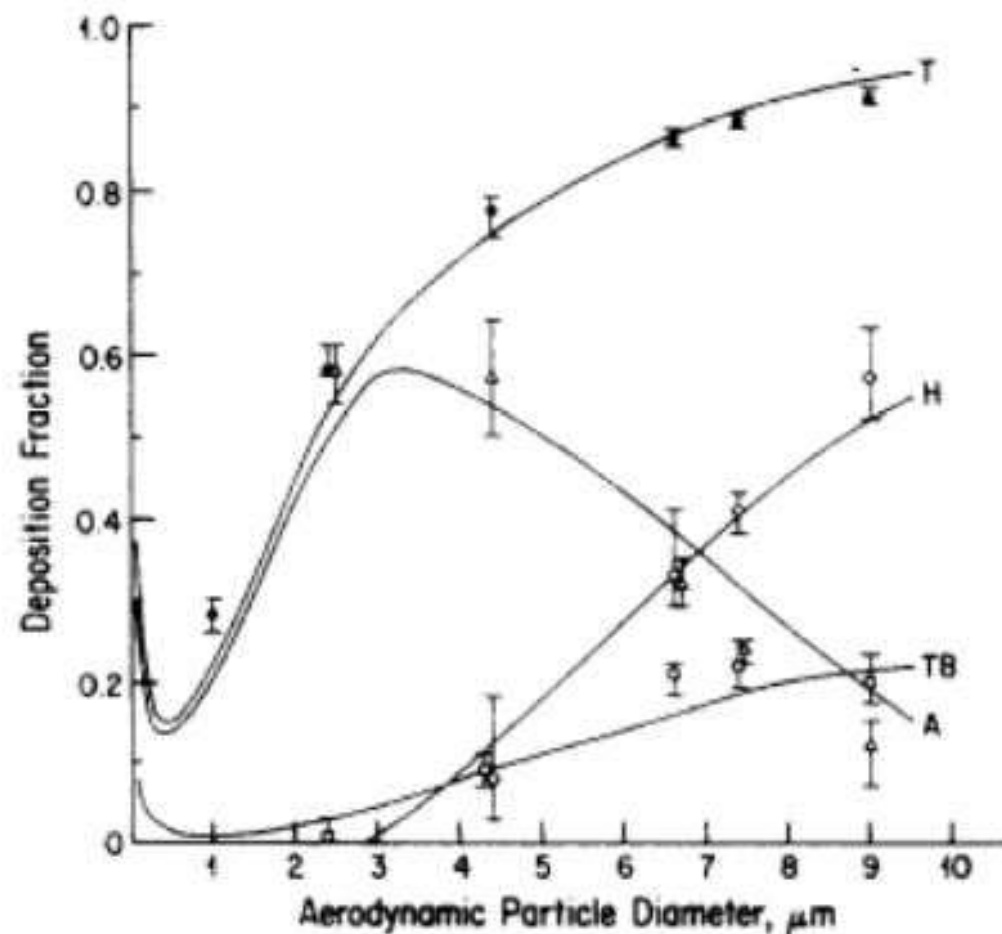
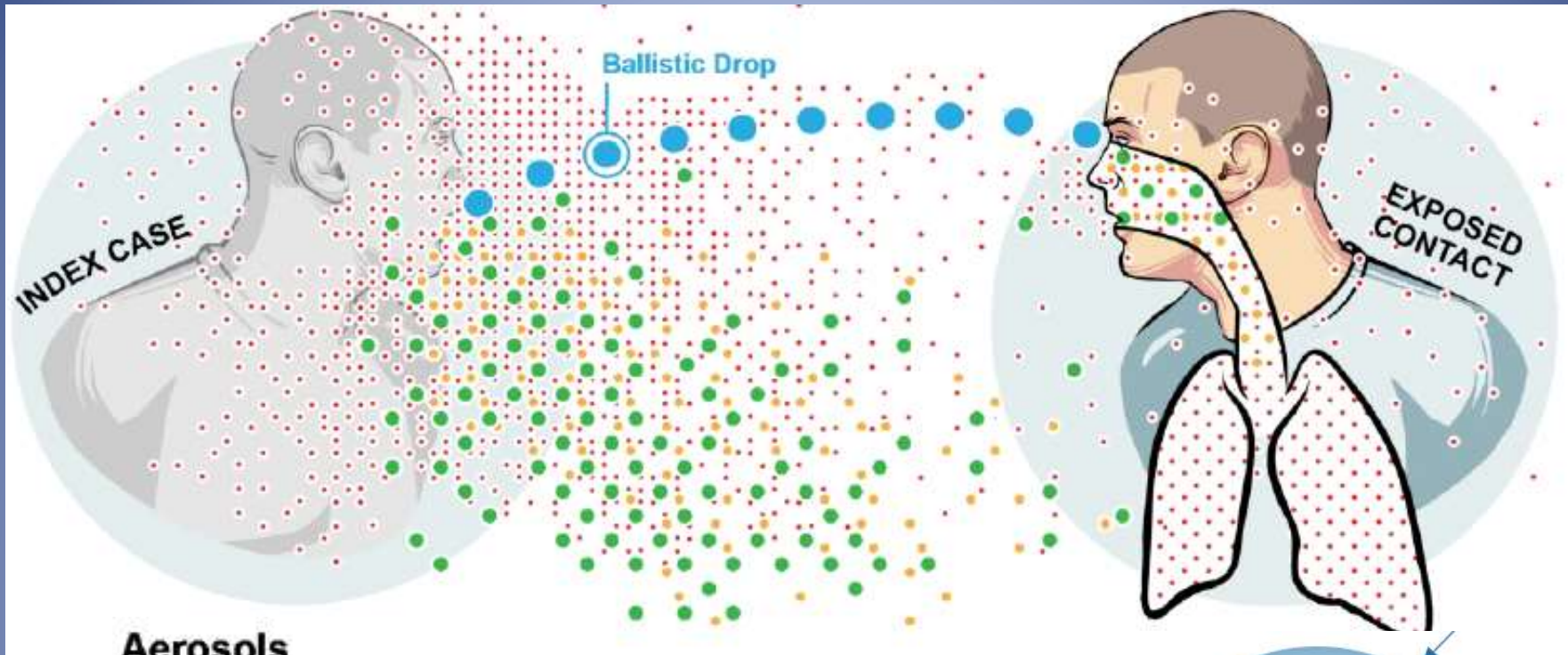


Fig. 13. Regional deposition as a function of aerodynamic particle diameter at mouth breathing for $Q = 250 \text{ cm}^3/\text{sec}$ and $\tau = 4 \text{ sec}$. The solid lines are the calculated values for head (H), tracheobronchial (TB), alveolar (A) and total (T) deposition.



Aerosols



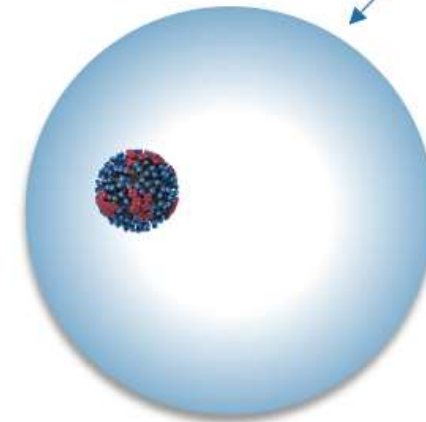
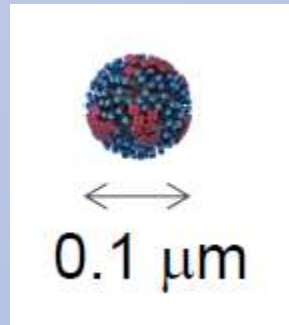
Respirable Aerosol
 ≤ 2.5 to $5\mu\text{m}$



Thoracic Aerosol
 ≤ 10 to $15\mu\text{m}$



Inhalable Droplets
 $\leq 100\mu\text{m}$



$(0.2-100\ \mu\text{m})$

Aérosols et transmission sur de longues distances

- Les aérosols peuvent être emportés très loin par des courants aériens ou des turbulences.
- Le risque d'infections sur de longues distances est modulé par la dilution, l'évacuation par la ventilation, la quantité émise à la source, , la dose infectieuse requise, et le déclin de l'infectivité .
- Une faible fréquence d'infections à longue distance peut être difficile à démontrer , et particulièrement pour des maladies communes dans la communauté.

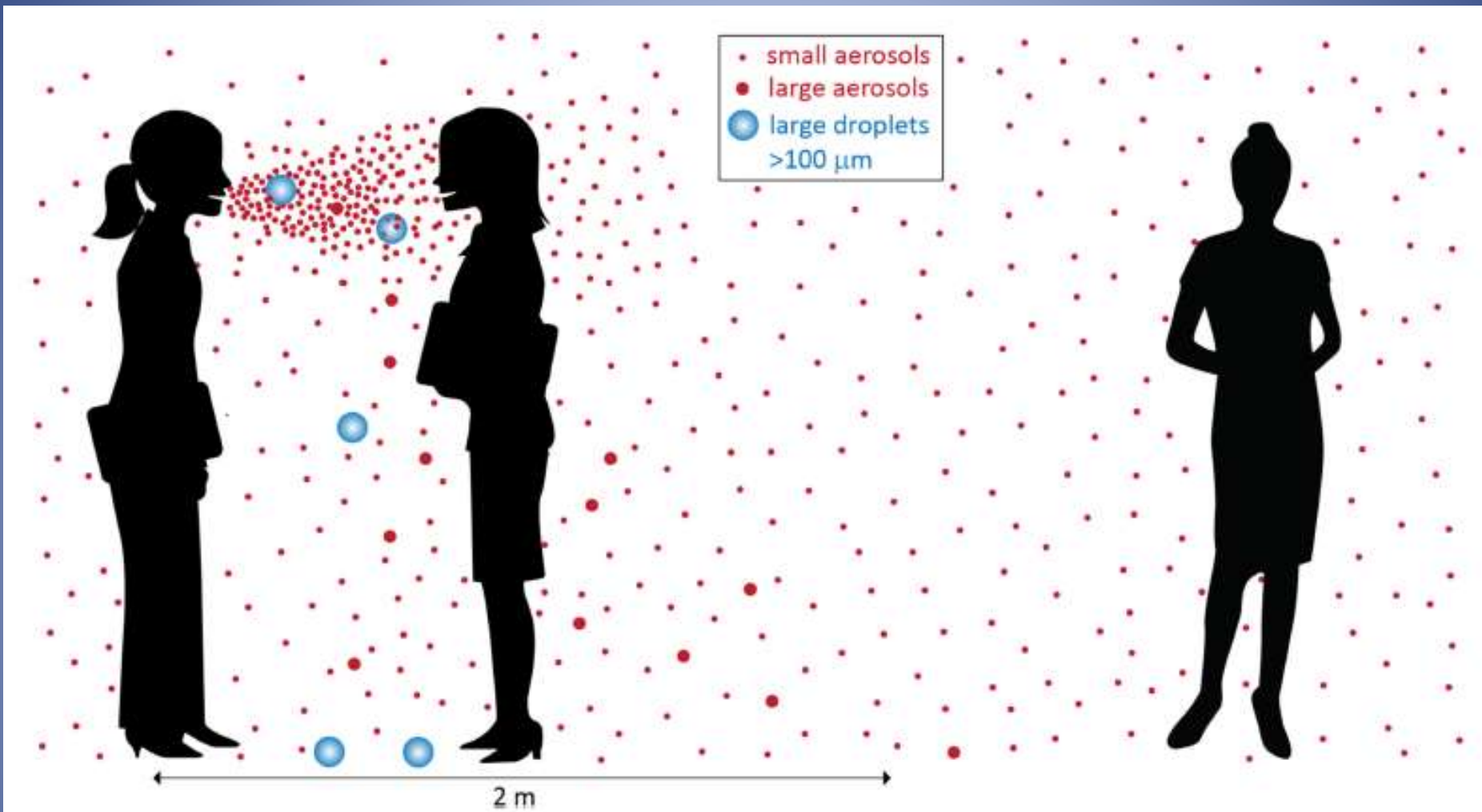


FIGURE 1 Illustration of droplets and aerosols released during talking; these may carry viruses if the person is infected. The large droplets fall rapidly to the ground in close proximity. The small aerosols are much more concentrated in close proximity, and they can remain floating in the air and spread throughout the room, leading to (reduced) exposure at a distance. Adapted from Tang et al⁹¹

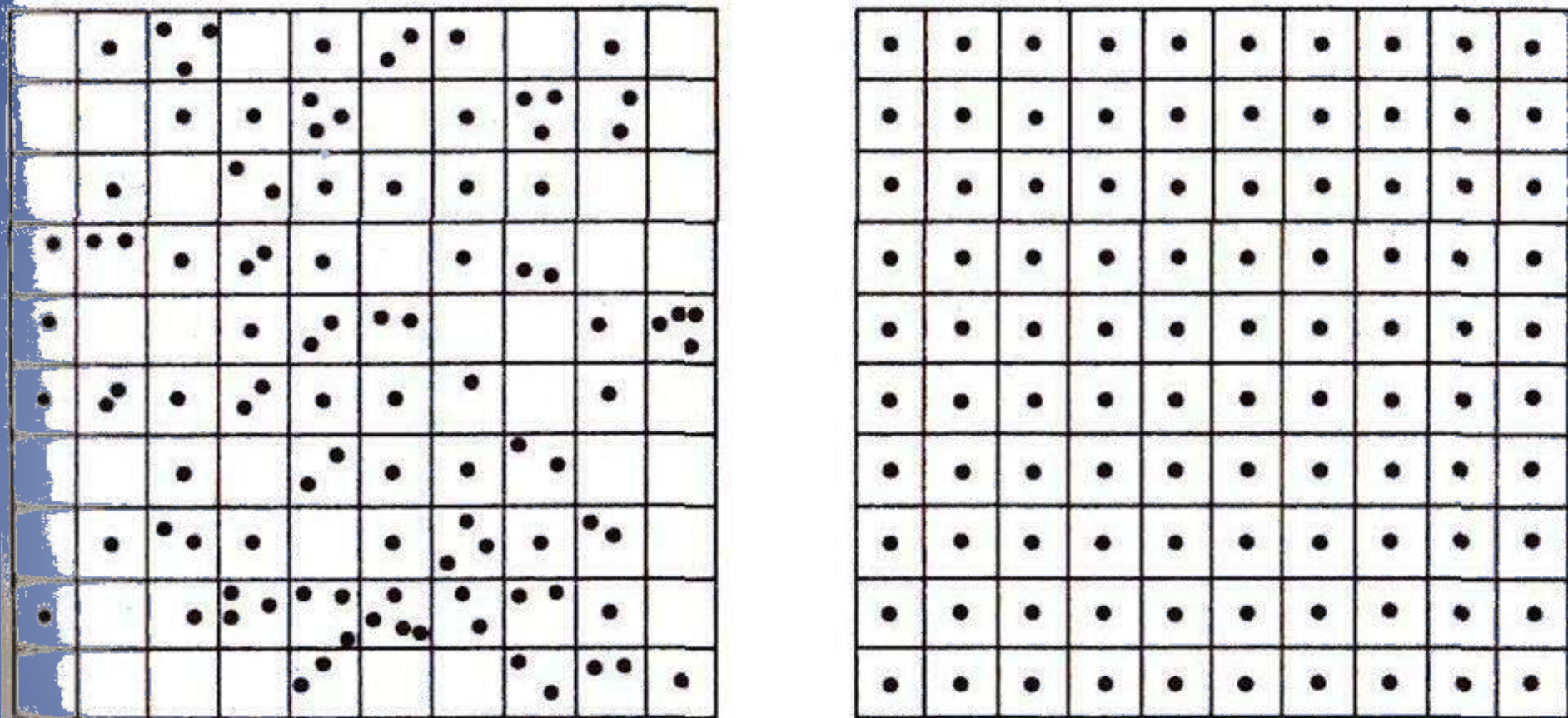
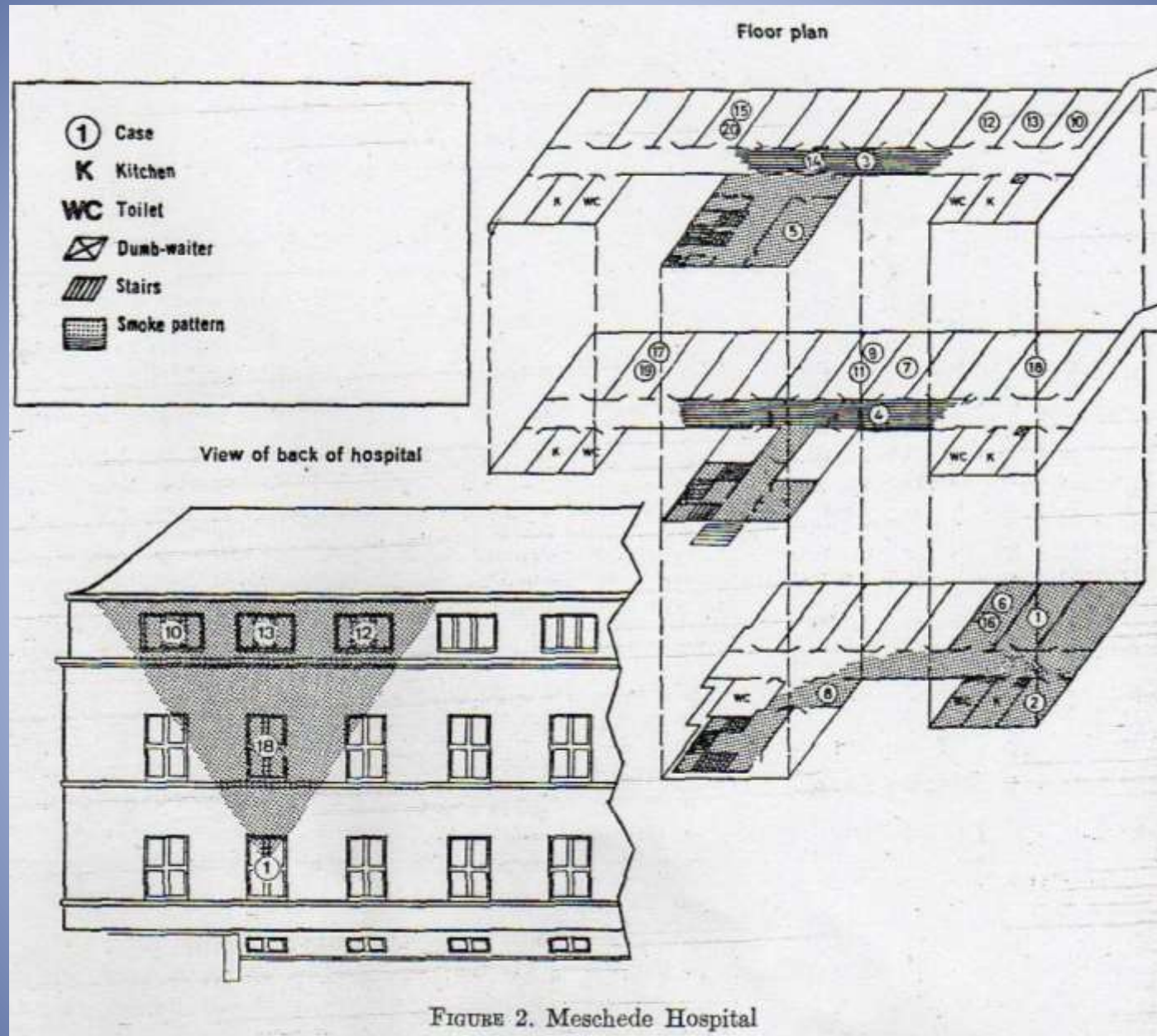


Fig. 21. Random vs. even distribution.

Riley RL, O' Grady F. Airborne Infection Transmission and Control
Macmillan New York 1961



Short-range airborne route dominates exposure of respiratory infection during close contact

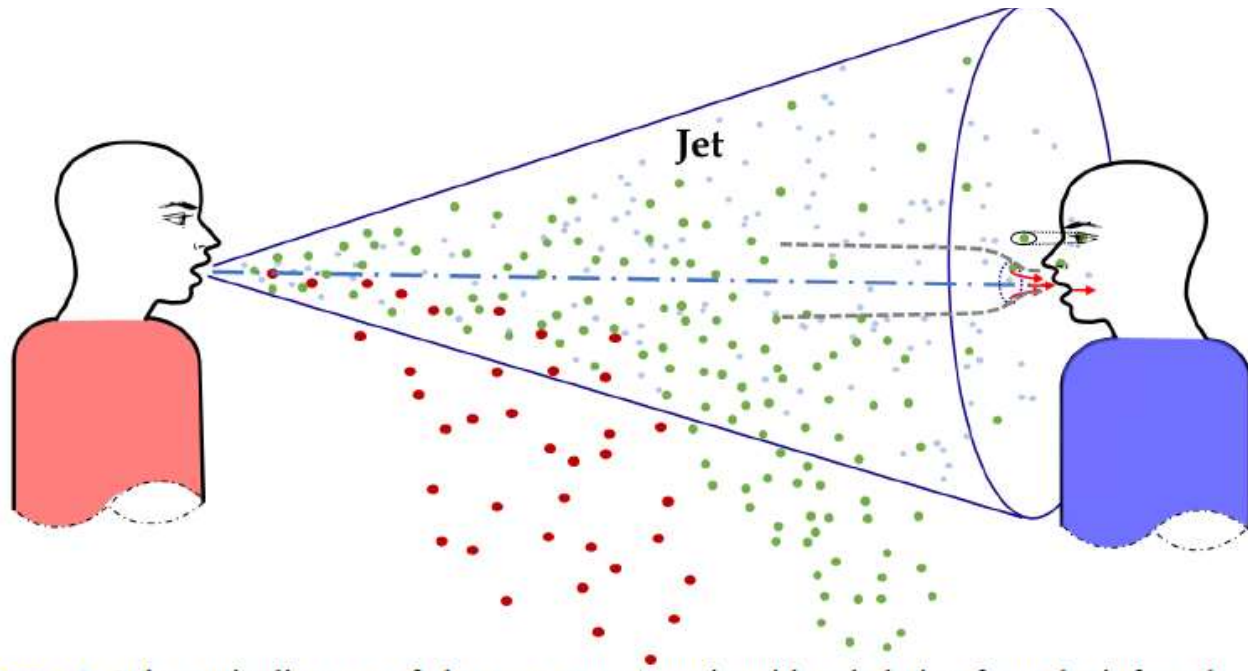


Figure 1. Schematic diagram of close contact scenario with exhalation from the infected (left) and inhalation through the mouth of the susceptible person (right).

Chen W et al
Building and Environment
vol 176 June 2020 106859

This is probably the first study in which the large droplet route, traditionally believed to be dominant, has been shown to be negligible compared to the short-range airborne route...

Short range airborne transmission is dominant beyond 0.2 m for talking and 0.5 m for coughing...

The work presented here poses a challenge to the traditional belief that large droplet infection is dominant.

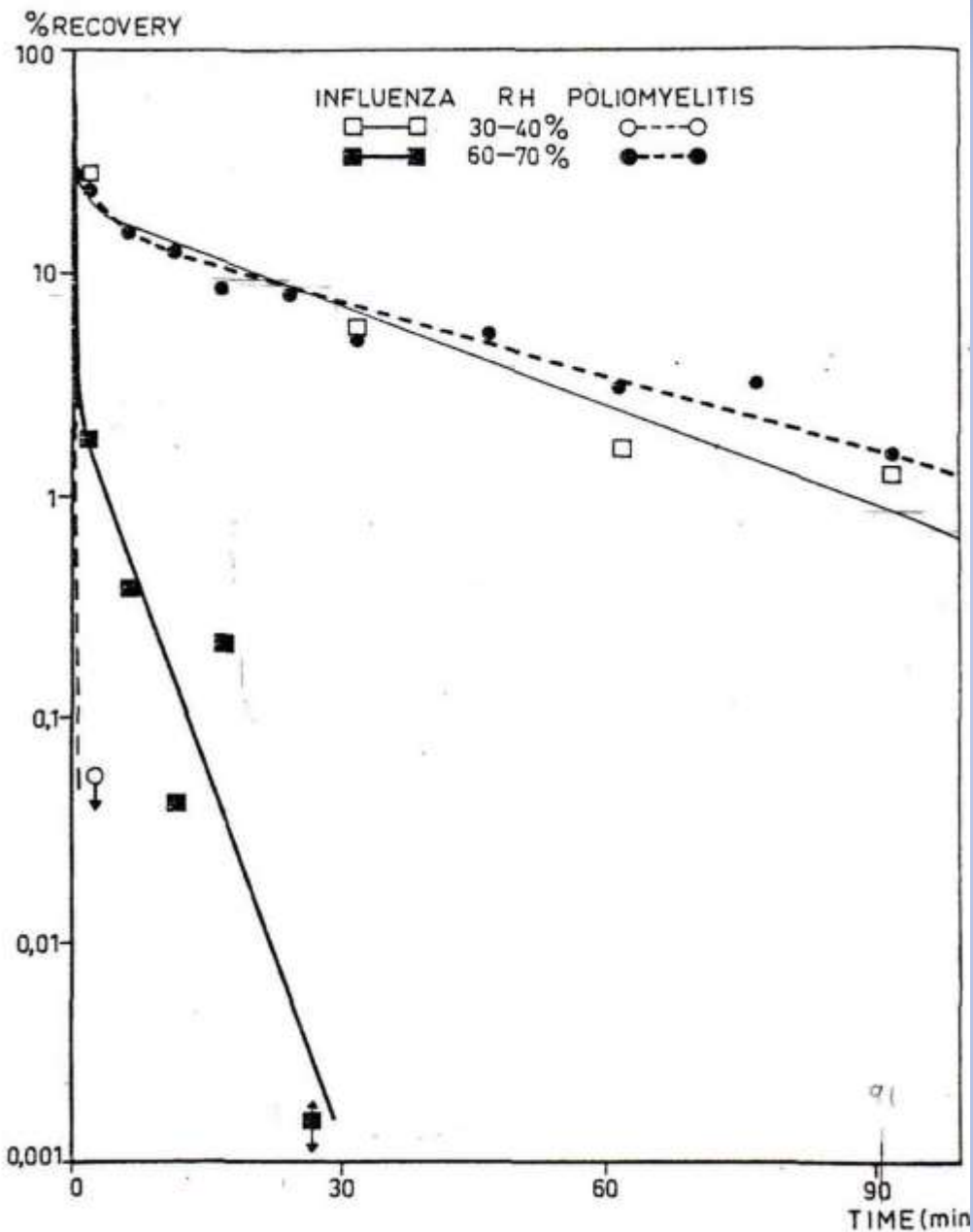


Fig. 6. Survival curves of poliomyelitis (CsL) and influenza (PR₈) virus, aerosolized in mixed suspensions at 20° C.

Hemmes et al 1962; Antonie Van Leeuwenhoek 1962; 28: 221-233

Median diameter:
5-6 μm



Milton DK et al ; PLOS One 2013;
6:e1003205

Table 2. Influenza virus type, results for each qPCR replicate, and exhalation rate.

Subject ID	Influenza virus type (sub-type)	qPCR of Filter Extract ^a			Influenza virus RNA exhalation rate ^b
		Replicate 1	Replicate 2	Replicate 3	
A-06	A (H3)	47	21	44	20
A-07	A (H3)	ND	ND	<6	<3.2
A-08	B	ND	ND	ND	ND
A-11	B	ND	ND	ND	ND
A-21	A (H3)	ND	ND	ND	ND
A-23	A (H3)	ND	ND	<6	<3.2
A-24	B	ND	7	ND	<3.2
A-25	B	ND	ND	ND	ND
A-34	B	ND	ND	ND	ND
B-01	A (H3)	ND	ND	ND	ND
B-09	B	ND	ND	ND	ND
B-25	B	ND	ND	ND	ND
A-37 (control)		ND	ND	ND	ND
A-38 (control)		ND	ND	ND	ND

^aNumber of influenza RNA copies detected per well (5 µl cDNA per well).

^bInfluenza virus RNA copies/ minute

ND = not detected by qPCR; limit of quantification was 6 influenza virus RNA copies per qPCR well when all three replicates were detected.

doi:10.1371/journal.pone.0002691.t002

Fabian P et al PLoS One 2008;
3: e2691

60% of patients with
Influenza A have detectable
viral RNA
14% of patients with
Influenza B have detectable
viral RNA

< 0.1% of particles
were > 5µm
(rarely recorded);
87% were < 1 µm

Table 3. Copy number coarse and fine exhaled particles without surgical mask by day since onset of influenza symptoms.

Days Since Onset ^a	Particle Size	Number of Cases	Number of Virus Particles		
			Min	Median	Maximum
1	Swab	10	2.1×10^4	1.1×10^6	3.4×10^7
	Coarse		<LD	2.3×10^1	2.9×10^4
	Fine		4	6.1×10^2	1.3×10^5
2	Swab	15	1.7×10^4	1.0×10^5	3.4×10^6
	Coarse		<LD	<LD	4.7×10^2
	Fine		<LD	2.1×10^1	3.9×10^4
3	Swab	7	2.3×10^4	1.4×10^6	1.0×10^7
	Coarse		<LD	<LD	1.1×10^2
	Fine		2	3.7×10^1	5.3×10^2
4	Swab	3	8.1×10^4	4.2×10^5	1.5×10^6
	Coarse		<LD	<LD	<LD
	Fine		3.2×10^1	7.5×10^1	4.4×10^2

^aBecause there were only single cases studied on day 0 (day of onset) and on day 5 since onset of symptoms, only data for cases studied on days 1 through 4 after onset of symptoms are shown.

doi:10.1371/journal.ppat.1003205.t003

Culture virale vs détection moléculaire (PCR): l'exemple du virus Influenza A

- Influenza A
1 TCID₅₀ = 100 -650 copies génomiques
- Impacteurs à haute vitesse utilisés pour collecter les aérosols endommagent les virions et abolissent leur infectivité.

Measurements of Airborne Influenza Virus in Aerosol Particles from Human Coughs

William G. Lindsley^{1*}, Françoise M. Blachere¹, Robert E. Thewlis¹, Abhishek Vishnu², Kristina A. Davis³, Gang Cao¹, Jan E. Palmer⁴, Karen E. Clark⁴, Melanie A. Fisher³, Rashida Khakoo³, Donald H. Beezhold¹

Table 1. Influenza viral RNA detected in the NIOSH two-stage aerosol sampler.

<i>Aerosol particle size range (aerodynamic diameter)</i>	<i>Median # of viral copies per cough</i>	<i>% of viral RNA contained in particles in this size range</i>	<i>% of subjects whose cough aerosol contained viral RNA-laden particles in this size range</i>
>4 μm	6.3 (SD 9.0)	35%	90%
1 to 4 μm	3.3 (SD 6.9)	23%	81%
<1 μm	3.7 (SD 23.7)	42%	75%
All particles	15.8 (SD 29.3)	100%	100%

Table 2. Viral plaque assay results for cough-generated aerosols.

<i>Aerosol sampler</i>	<i>Total # of subjects for whom VPA was performed on cough aerosol</i>	<i>Total # of these subjects who were influenza-positive (by qPCR or VPA)</i>	<i># of influenza-positive nasal swabs</i>		<i># of influenza-positive cough aerosols</i>	
			<i>qPCR</i>	<i>VPA</i>	<i>qPCR</i>	<i>VPA</i>
NIOSH two-stage sampler	20	12	9 (of 18)	7	8	1
SKC BioSampler	10	9	9	4	6	1

Nasopharyngeal swabs and cough aerosol samples from 30 subjects were cultured for viable influenza virus. This table shows the number of samples found to be influenza-positive by qPCR and VPA.

Variable	NP swab	Coarse aerosol	Fine aerosol
Culture passage			
Valid assays	169	NA	134
Positive (%)	150 (89)	NA	52 (39)
Quantitative culture (FFU)			
Valid assays	159	NA	136
Positive (%)	98 (62)	NA	41 (30)
GM (GSD)	2.5×10^3 (23)	NA	37 (4.4)
Range	ND – 5.1×10^5	NA	ND – 1.1×10^3
RNA copies			
Valid assays	218	218	218
Positive (%)	211 (97)	88 (40)	166 (76)
GM (GSD)	8.2×10^8 (52)	1.2×10^4 (14)	3.8×10^4 (13)
Range	ND – 3.8×10^{11}	ND – 4.3×10^8	ND – 4.4×10^7

GSD, geometric SD (only positive samples were included in computation of GM and GSD); NA, not assayed; ND, not detected.

Infectious virus in exhaled breath of symptomatic seasonal influenza cases from a college community

Jing Yan^{a,b}, Michael Grantham^{a,1}, Jovan Pantelic^{a,2}, P. Jacob Bueno de Mesquita^a, Barbara Albert^a, Fengjie Liu^{a,3}, Sheryl Ehrman^{b,4}, Donald K. Milton^{a,5}, and EMIT Consortium⁶

Table 1. Clinical investigation of airborne influenza in a hospital emergency department.

Day	No. of patients reporting influenza-like symptoms	Total no. of stationary samplers	Total no. of personal samplers	Samplers showing results positive for influenza virus	No. of TCID ₅₀ -equivalent RNA particles detected in the sampler			
					First stage	Second stage	Filter	Total
1	4	9	4	Waiting room (lower sampler)	460	0	0	460
				Waiting room (upper sampler)	0	13,426	2852	16,278
				Reception and triage room	0	1941	0	1941
				Personal sampler (physician 1)	3160	0	0	3160
				Personal sampler (physician 2)	309	0	0	309
				Personal sampler (physician 3)	0	4623	0	4623
2	0	13	0	Waiting room, (upper sampler)	1114	0	0	1114
3	5	13	1	None
4	3	13	0	Children's waiting room (lower sampler)	4025	11,040	0	15,065
				Children's waiting room (upper sampler)	5762	<100	0	5762
				Waiting room (lower sampler)	15,532	0	0	15,532
				Waiting room (lower sampler)	0	1367	0	1367

First stage: > 4 μ m
2nd stage: 1-4 μ m
Filter: < 1 μ m

Blachere et al CID 2009; 48: 438-440

Table 3. Average ambient relative humidity and temperature and total airborne influenza A virus concentration in each of 16 samples. Humidity and temperature were recorded every 2 min, and each sample was collected using a cascade impactor for 6–8 h. IAV RNA was extracted from filters and quantified by qRT-PCR. It was not detected in half of the samples. In the samples containing detectable amounts of IAV, the average concentration was $1.6 \pm 0.9 \times 10^4$ genome copies m^{-3} .

date	location	RH (%)		temperature ($^{\circ}C$)		total IAV concentration (genome copies m^{-3})	
		mean	s.d.	mean	s.d.	mean	s.d.
10 Dec 2009	health centre	16.98	1.71	21.17	0.25	1.6×10^4	1.2×10^4
17 Dec 2009	day-care	42.93	2.85	20.71	0.36	1.6×10^4	1.0×10^4
30 Dec 2009	aeroplane	n.a. ^a	n.a.	n.a.	n.a.	n.d. ^b	n.d.
26 Jan 2010	health centre	21.72	0.89	20.75	0.54	n.d.	n.d.
27 Jan 2010	day-care	32.93	2.03	25.12	1.06	3.7×10^4	2.0×10^3
9 Feb 2010	health centre	25.15	0.80	20.86	0.56	5.8×10^3	6.2×10^2
11 Feb 2010	health centre	18.77	1.13	20.51	0.68	n.d.	n.d.
22 Mar 2010	aeroplane	29.25	13.86	25.11	3.47	1.4×10^4	1.0×10^3
24 Mar 2010	aeroplane	25.06	8.69	21.85	1.37	1.1×10^4	1.1×10^3
30 Mar 2010	health centre	29.81	4.83	22.16	0.85	n.d.	n.d.
31 Mar 2010	day-care	43.61	1.58	21.82	0.85	1.6×10^4	1.1×10^2
6 Apr 2010	health centre	54.66	5.00	23.15	0.75	1.5×10^4	1.7×10^3
8 Apr 2010	health centre	49.33	1.15	22.71	0.37	n.d.	n.d.
9 Apr 2010	day-care	52.12	0.82	22.02	1.01	n.d.	n.d.
20 Apr 2010	health centre	31.70	1.07	21.84	0.86	n.d.	n.d.
22 Apr 2010	health centre	32.53	2.29	21.91	0.75	n.d.	n.d.

^aNot available owing to a logging error.

^bNo detectable influenza A virus genome.

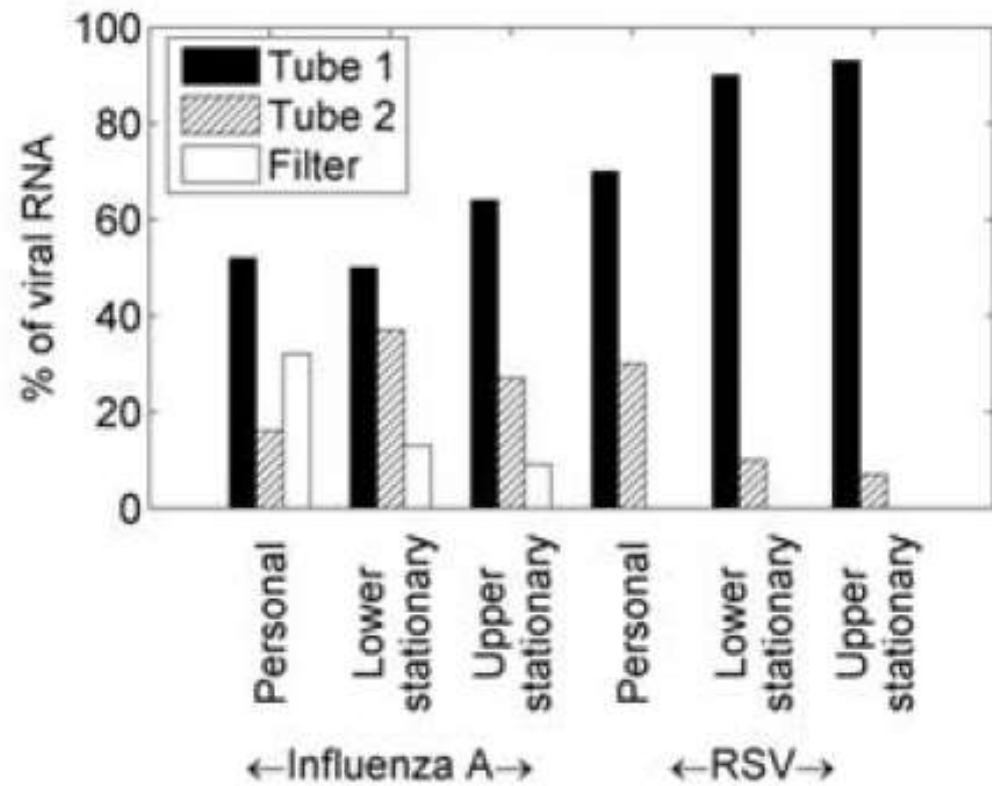
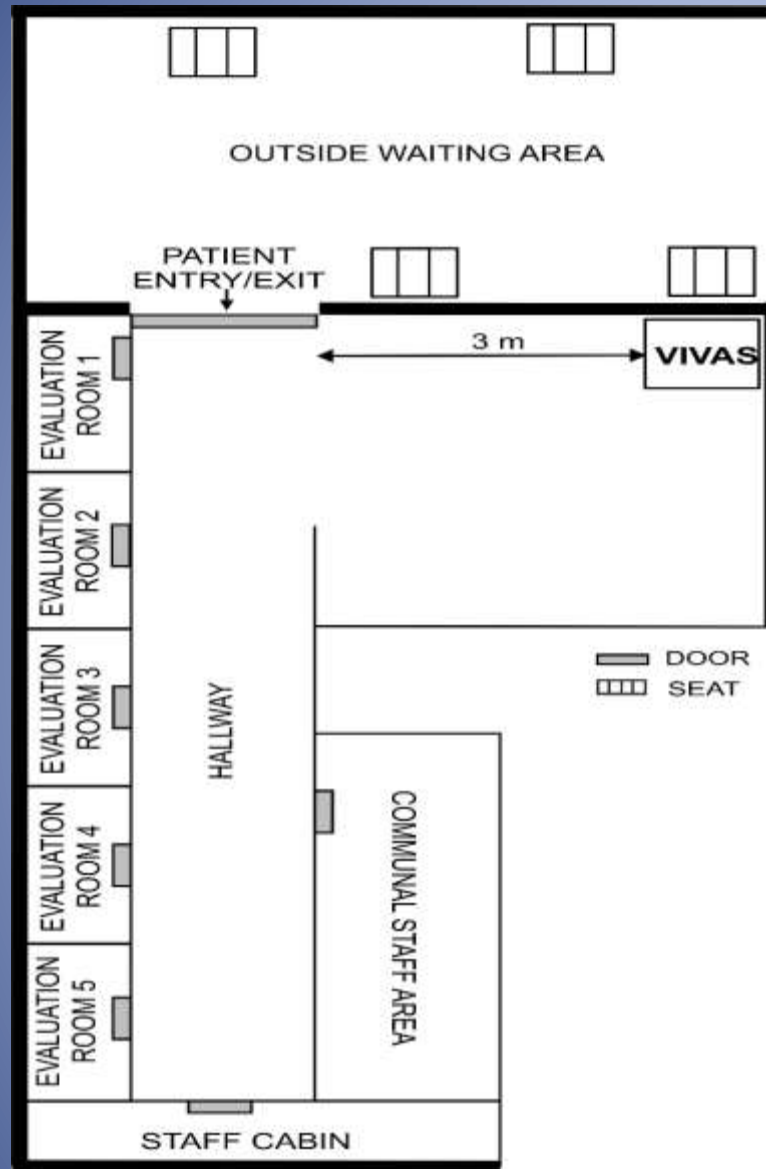


Figure 2. Distribution of viral RNA within samplers. Aerosol size ranges for stationary samplers were: tube 1, particles $\geq 4.1 \mu\text{m}$ aerodynamic diameter; tube 2, $1\text{--}4.1 \mu\text{m}$; filter, $\leq 1 \mu\text{m}$. Because they operated at a lower flow rate, the collection size fractions for the personal samplers were slightly larger: tube 1 contained particles $\geq 4.9 \mu\text{m}$; tube 2, $1.7\text{--}4.9 \mu\text{m}$; filter, $\leq 1.7 \mu\text{m}$.



Aerosol and Air Quality Research, 20: 1167–1171, 2020
 Publisher: Taiwan Association for Aerosol Research
 ISSN: 1680-8584 print / 2071-1409 online
<https://doi.org/10.4209/aaqr.2020.05.0202>

Collection of SARS-CoV-2 Virus from the Air of a Clinic within a University Student Health Care Center and Analyses of the Viral Genomic Sequence

John A. Lednicky^{1,2}, Sripriya N. Shankar³, Maha A. Elbadry^{1,2}, Julia C. Gibson^{1,2},
 Md. Mahbulul Alam^{1,2}, Caroline J. Stephenson^{1,2}, Arantzazu Eiguren-Fernandez⁴,
 J. Glenn Morris^{2,5}, Carla N. Mavian^{2,6}, Marco Salemi^{2,6}, James R. Clugston^{7,8},
 Chang-Yu Wu^{3*}

Run Summary

Sample ID: 032720Air1ME1	Run Date: 16 Apr 2020 9:21 AM
Detected: Coronavirus OC43 Influenza A H1-2009 Influenza A H3	Controls: Passed
Equivocal: None	

Result Details

Result	Interpretation	Call	Assay
Not Detected	Adenovirus	Negative Negative	Adeno Adeno2
Not Detected	Coronavirus 229E	Negative	CoV-229E
Not Detected	Coronavirus HKU1	Negative	CoV-HKU1
Not Detected	Coronavirus NL63	Negative	CoV-NL63
✓ Detected	Coronavirus OC43	Positive	CoV-OC43
Not Detected	Human Metapneumovirus	Negative	hMPV
Not Detected	Human Rhinovirus/Enterovirus	Negative Negative Negative Negative Negative	Entero1 Entero2 HRV1 HRV2 HRV3 HRV4
✓ Detected ✓ Detected	Influenza A H1-2009 Influenza A H3	Positive Positive Positive Negative Positive	FluA-H1-2009 FluA-H1-pan FluA-H3 FluA-pan1 FluA-pan2
Not Detected	Influenza B	Negative	FluB
Not Detected	Parainfluenza Virus 1	Negative	PIV1
Not Detected	Parainfluenza Virus 2	Negative	PIV2
Not Detected	Parainfluenza Virus 3	Negative	PIV3
Not Detected	Parainfluenza Virus 4	Negative	PIV4
Not Detected	Respiratory Syncytial Virus	Negative	RSV
Not Detected	<i>Bordetella pertussis</i>	Negative	Bper
Not Detected	<i>Chlamydia pneumoniae</i>	Negative	Cpne
Not Detected	<i>Mycoplasma pneumoniae</i>	Negative	Mpne
Result	Control	Call	Assay
Pass	PCR2 Control	Positive	PCR2
Pass	RNA Process Control	Positive	yeastRNA

Fig. 2. Biofire RVP test results for viruses isolated after inoculation of Vero E6 cells with sample 1. Human coronavirus OC43, and Influenza A H1N1 and H3N2 viruses were identified.

Infections expérimentales avec l'influenza A chez des volontaires

- Les infections expérimentales permettent de séparer clairement la transmission par aérosols et par grosses gouttelettes.
- Un inoculat homogène d'aérosols sans grosses gouttelettes peut être préparé en laboratoire
- La transmission par grosse gouttelettes est simulée par les instillations intranasales, en l'absence d'aérosols.

TABLE I. Aerosol Administration of Influenza A2/Bethesda/10/63 to Volunteers.

Inhaled virus (TCID ₅₀)	Vol #	Illness	Virus recovery (days after inoc)	Neutralization antibody	
				Before inoculation	28 days after
126	1	*	*	1280	2560
	2			2560	2560
	3			640	1280
78	4			160	160
	5			320	320
	6			320	320
59	7			40	1280
	8			80	80
	9			80	80
1	10	+	3-7	<5	80
2	11			<5	<5
	12			<5	<5
	13			<5	<5
	14		4-7	<5	320
5	15			40	40
	16			80	80
	17			40	40
	18	+	4, 7	10	1280
	19			20	1280
	20	+	2-6	5	5120
	21			<5	<5
	22	+	2-6	<5	640
	23			<5	<5

* Blank spaces indicate no response.

Maladie clinique causée les infections expérimentales

- Par les aérosols: le spectre clinique est semblable à celui observé dans les infections naturelles, y compris les cas sévères.
- Par instillation intranasale, la maladie est plus bénigne et épargne les voies respiratoires inférieures.

- 1) Douglas R.G. Influenza in Man. Pp 375-447 in The Influenza Viruses and Influenza, Kilbourne E.D. ed, Academic Press, New York 1975
- 2) Little J.W. et al J Med Virol 3: 177-188, 1979.
- 3) Knight V.pp. 175-182 in: Hers JF, Winkles KC, eds. Airborne Transmission and Airborne Infections VIth International Symposium on Aerobiology. New York: Wiley; 1973

Comparaison des doses infectieuses requises

- Aerosol:

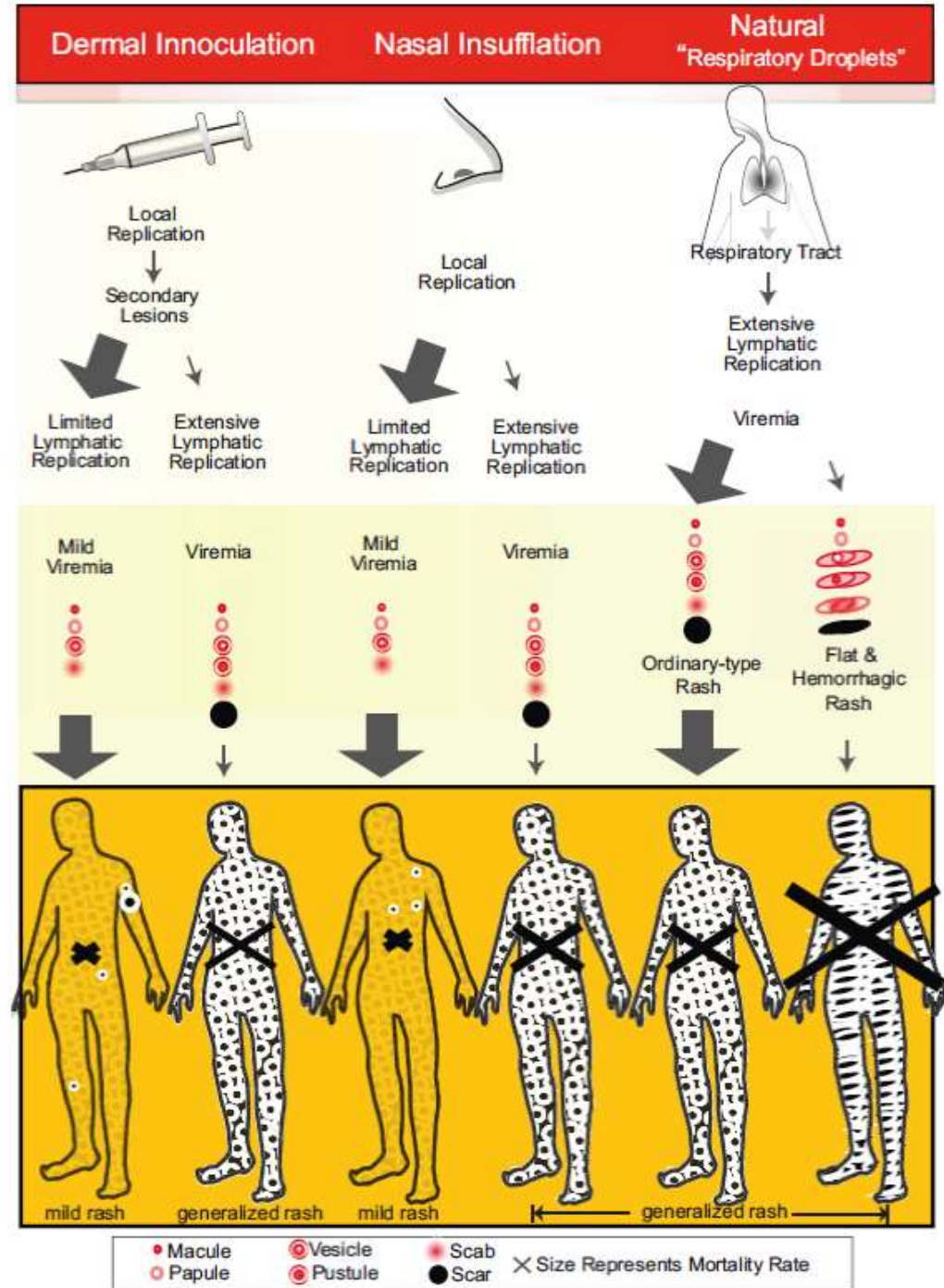
$$\text{HID}_{50} = 0.6 \text{ to } 3 \text{ TCID}_{50}$$

- Instillation intranasale

$$\text{HID}_{50} = 127 \text{ to } 320 \text{ TCID}_{50}$$

(Douglas R.G. Influenza in Man. Pp 375-447 in
The Influenza Viruses and Influenza, Kilbourne E.D. ed,
Academic Press, New York 1975.)

Milton DK Cellular
and Infection Microbiology
published: 29 November 2012
doi: 10.3389/fcimb.2012.00150



Anisotropic Infection

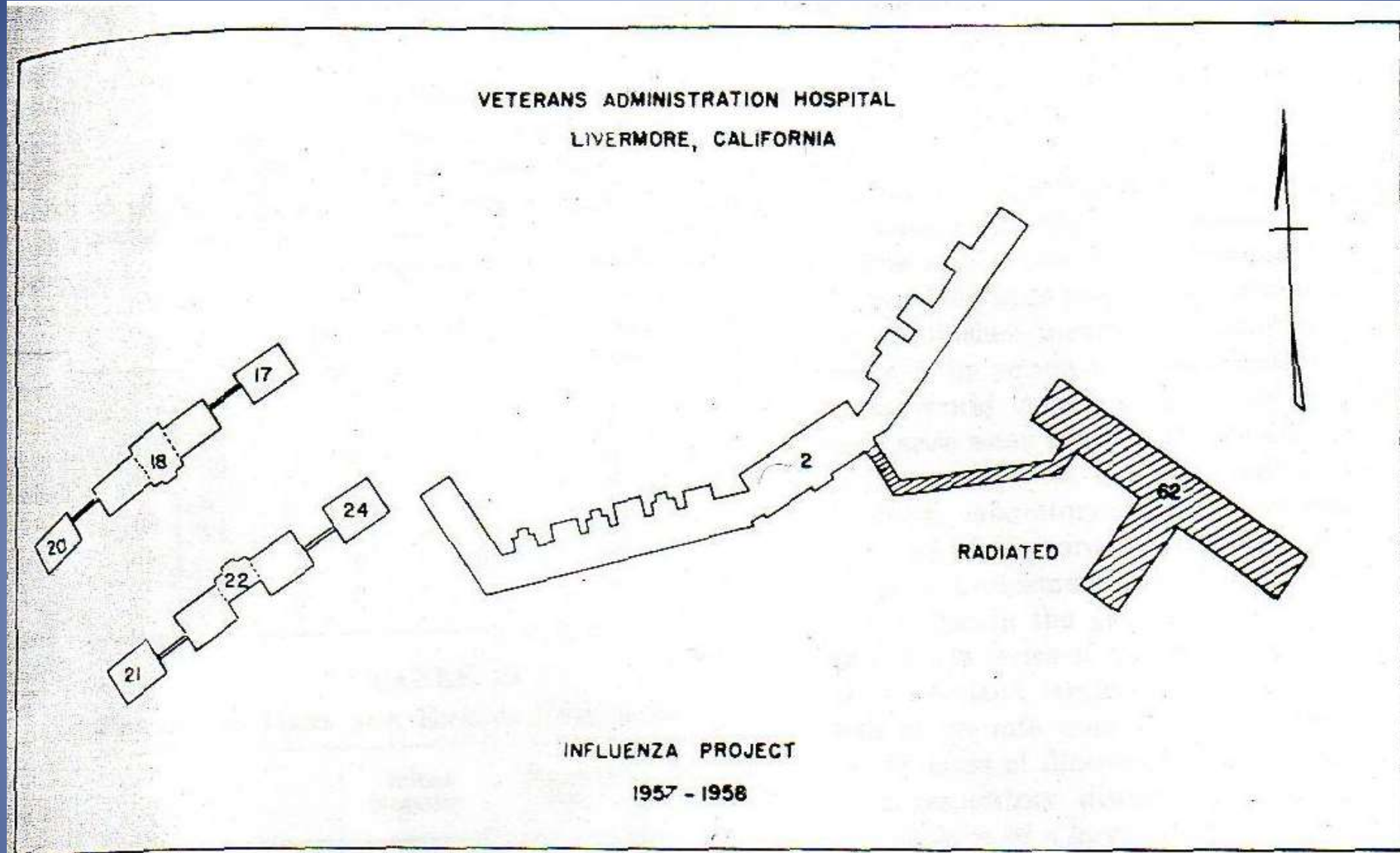
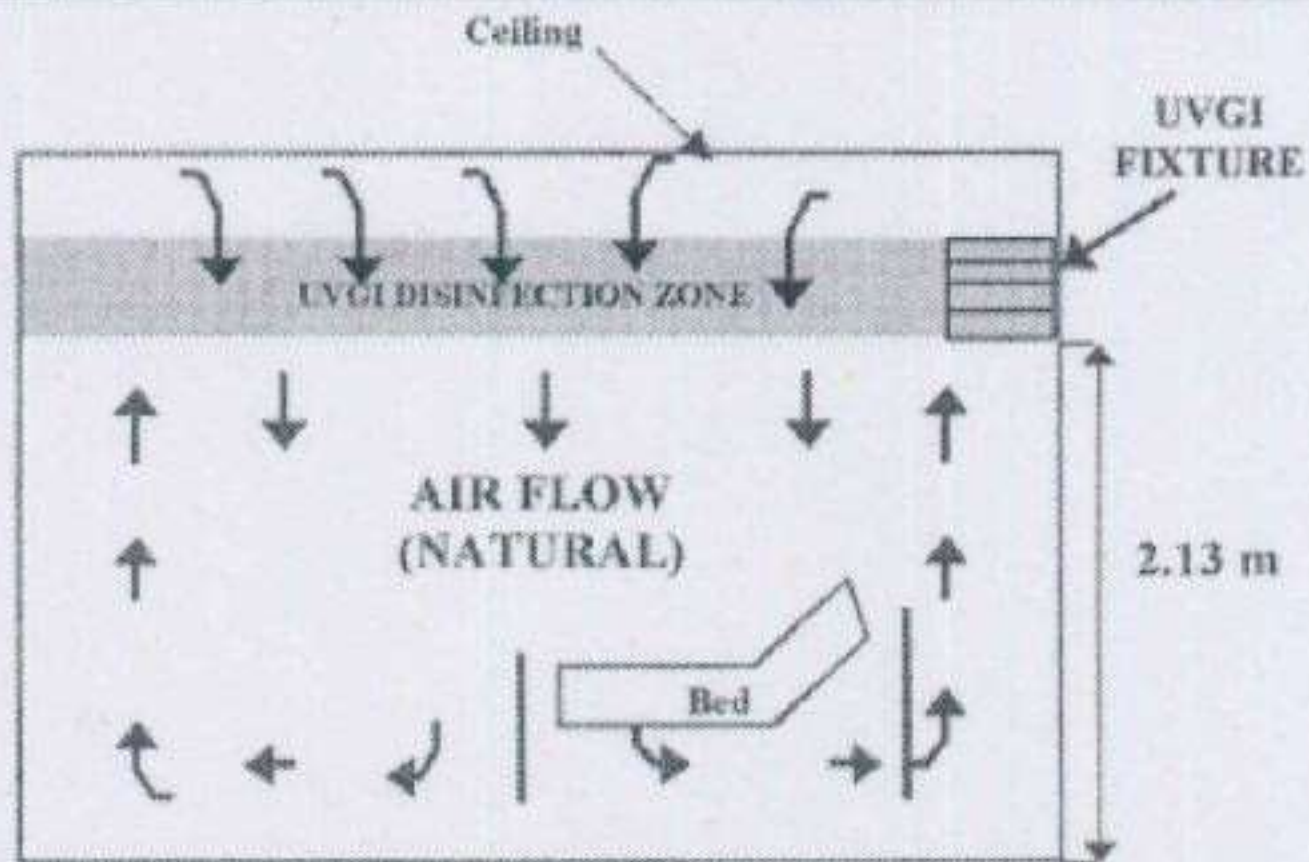


FIG. 4. Illustrates the plan of the hospital grounds and depicts the area which was isolated from the rest of the hospital by radiant disinfection of the upper air of all rooms and corridors.

Figure 3. Section view of wall-mounted UVGI fixture irradiating the upper room space over a hospital bed



Arrows indicate convection currents.

TABLE 9
 NUMBER OF PATIENTS WITH ACUTE
 RESPIRATORY SYMPTOMS
 Phase 2, November 16, 1957-March 16, 1958

Week of	Radiated		Nonradiated	
	Influenza	Other	Influenza	Other
12/15	0	0	2	0
12/22	0	1	1	5
12/29	0	0	0	8
1/5	0	2	7	4
1/12	0	0	18	6
1/19	0	0	10	4
1/26	0	1	1	1

TABLE 10
 SEROLOGIC DATA FOR ENTIRE PERIOD OF STUDY

	Initial Negative	Fourfold Rise	Per Cent Positive
Patients:			
Radiated.....	209	4	2
Nonradiated..	396	75	19
Personnel.....	511	92	18

Safety and efficacy of once daily intranasal zanamivir in preventing experimental human influenza A infection

David P Calfee¹, Amy W Peng², Elizabeth K Hussey², Monica Lobo¹ and Frederick G Hayden^{1*}

¹Department of Internal Medicine, University of Virginia Health Sciences Center, Charlottesville, Va., USA

²Glaxo Wellcome Inc., Research Triangle Park, N.C., USA

Table 4. Prevention of experimental infection with influenza A/Texas/91 (H1N1) with various intranasal zanamivir regimens

Study group	Number of subjects	Number (%) shedding virus	Number (%) with seroconversion	Number (%) with infection
Zanamivir 48 h prior to inoculation	12	6 (50)	7 (58)	8 (67)
Zanamivir 4 h prior to inoculation	12	1 (8)*	4 (33)	4 (33)
Zanamivir daily for 3 days	10	1 (10)†	0 (0)*	1 (10)† ←
Placebo	9	7 (78)	7 (78)	7 (78)

* $P < 0.005$ compared to placebo.

† $P < 0.05$ compared to placebo.

Short-Term Treatment with Zanamivir to Prevent Influenza: Results of a Placebo-Controlled Study

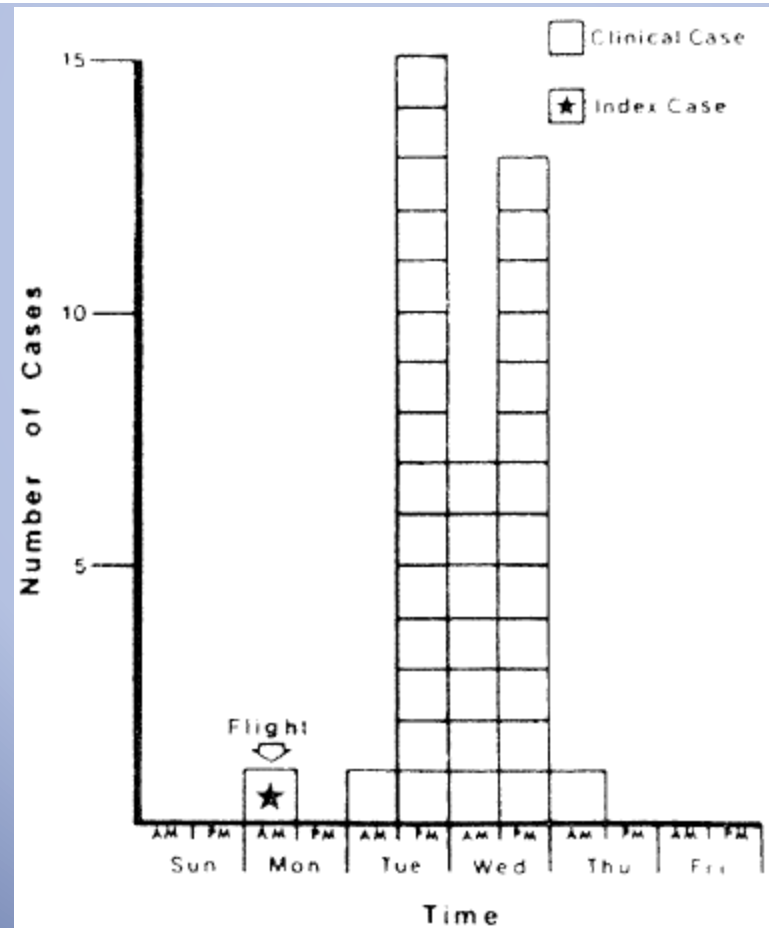
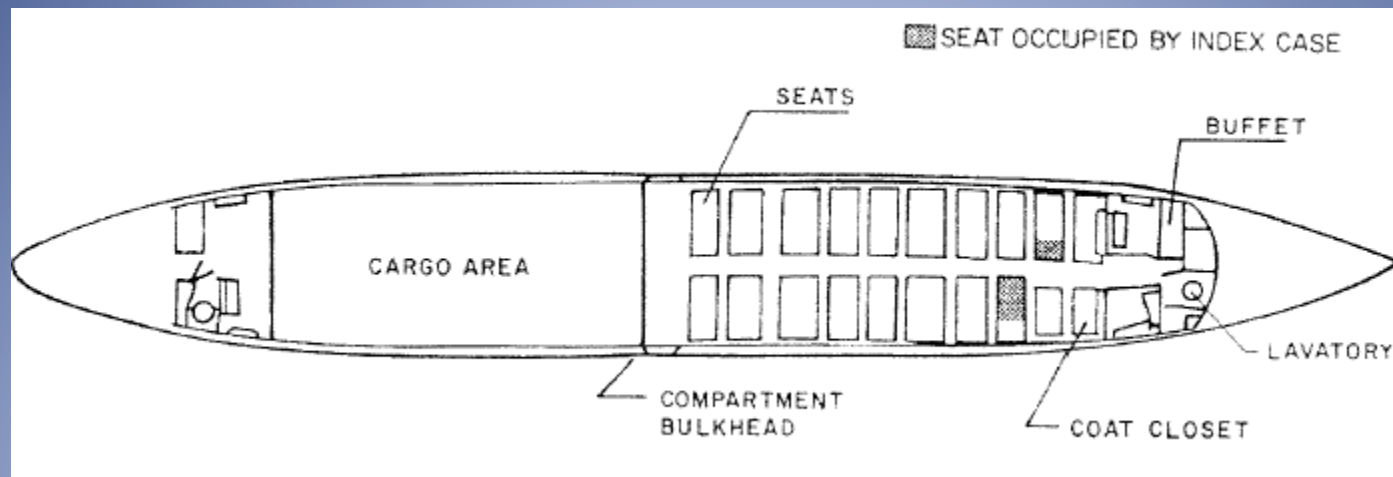
Laurent Kaiser,¹ Dan Henry,² Nancy P. Flack,³
Oliver Keene,⁴ and Frederick G. Hayden¹

From the ¹Division of Epidemiology and Virology, Department of Internal Medicine, University of Virginia School of Medicine, Charlottesville; ²Foothill Family Clinic, Salt Lake City, Utah; ³Glaxo Wellcome, Research Triangle Park, North Carolina; and ⁴Glaxo Wellcome Research and Development, Greenford, Middlesex, United Kingdom

Table 2. Incidence of symptomatic influenza (S) or asymptomatic influenza (AS) after initiation of prophylaxis, by treatment group.

	Placebo (n = 144)	Zanamivir			Total no. of subjects
		Intranasal (n = 141)	Inhaled (n = 144)	Intranasal and inhaled (n = 146)	
Proven influenza					
S or AS during 21 d after initiation	27 (19)	28 (20) ←	16 (11) ←	21 (14)	92
S during 10 d after initiation	11 (8)	9 (6)	4 (3)	6 (4)	30
OR (95% CI)		0.81 (0.30–2.22)	0.31 (0.09–1.04)	0.51 (0.17–1.49)	
S during 5 d of prophylaxis	9 (6)	8 (6) ←	3 (2) ←	5 (3)	25
OR (95% CI)		0.9 (0.30–2.72)	0.27 (0.07–1.05)	0.52 (0.17–1.58)	

NOTE. Data are no. (%) of subjects, except as indicated. ORs and 95% CIs stratified by center were calculated by use of Mantel-Haenszel estimates with test-based CIs.



37 cases
Attack rate 72%

Moser MR et al 1979;
AM J Epidemiol 110: 1-6

Gregg MB 1980;
NY Acad Sci 353: 45-53

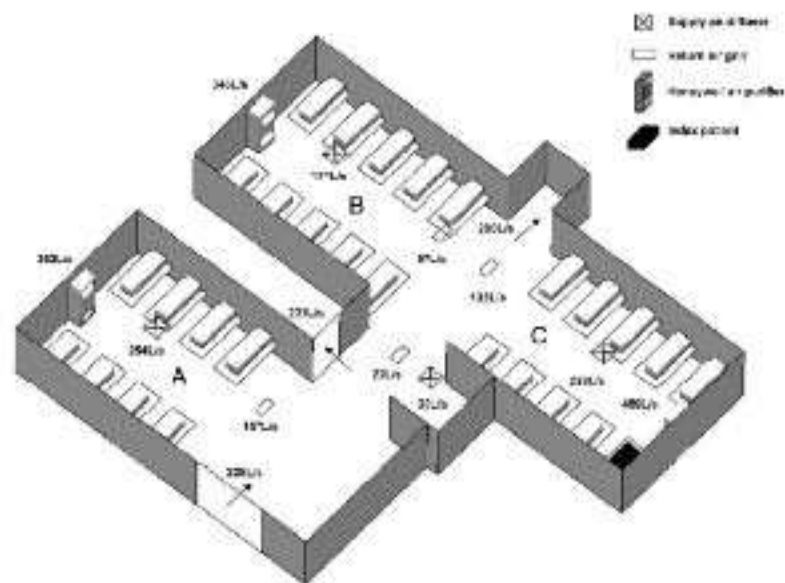
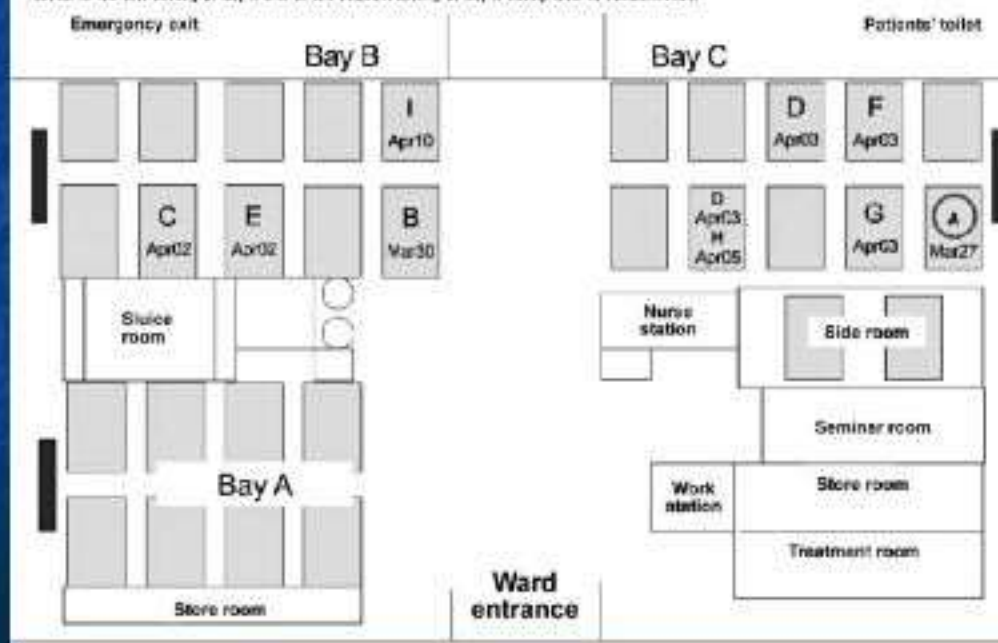


Figure 3. The measured airflow rates (in the unit of L/s) at different ward locations. High efficiency particulate absorbing (HEPA) air purifiers were turned to the low setting in bay B and to the medium setting in bay C during time of measurement.



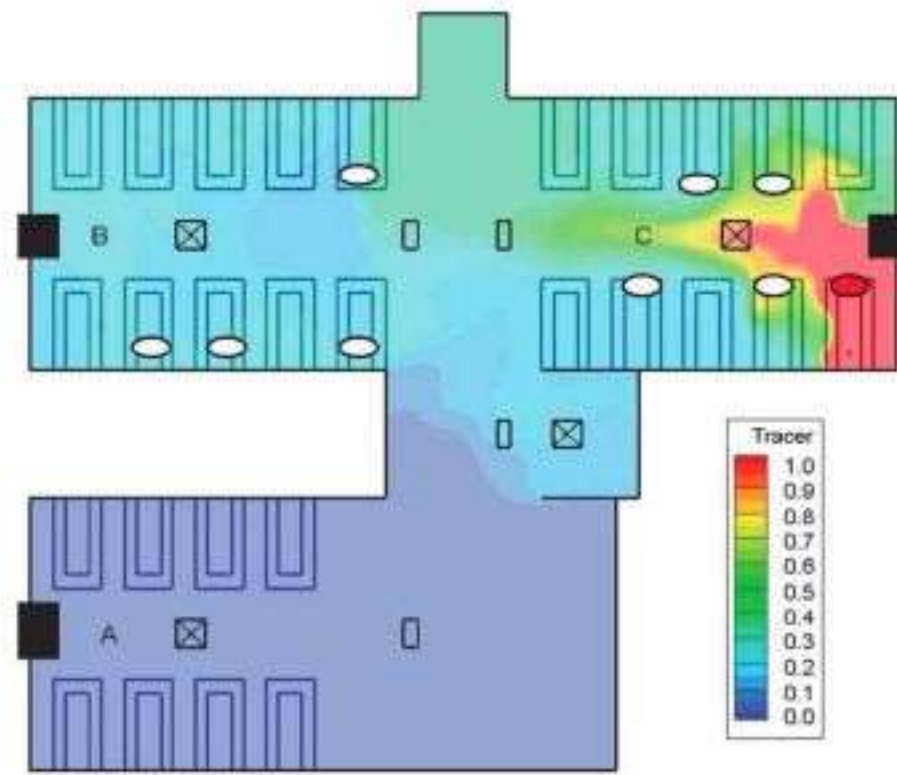


Figure 5. The spatial distribution of normalized concentration of hypothetical virus-laden aerosols (modeled as gaseous tracer) in the outbreak ward at a height of 1.1 m. The flow rates used in this model were those described in Figure 3. All high-efficiency particulate absorbing (HEPA) filters were assumed to function with 100% filtration of the modeled droplet nuclei. The 3 HEPA air purifiers are shown as black boxes, the 4 diffusers are shown by a square with an X, and the 4 returns are shown as a small rectangular filled box. Affected patients are represented by white ovals (the index patient is marked as a red oval).

Transmission entre animaux de l'influenza A par aérosols chez des espèces susceptibles

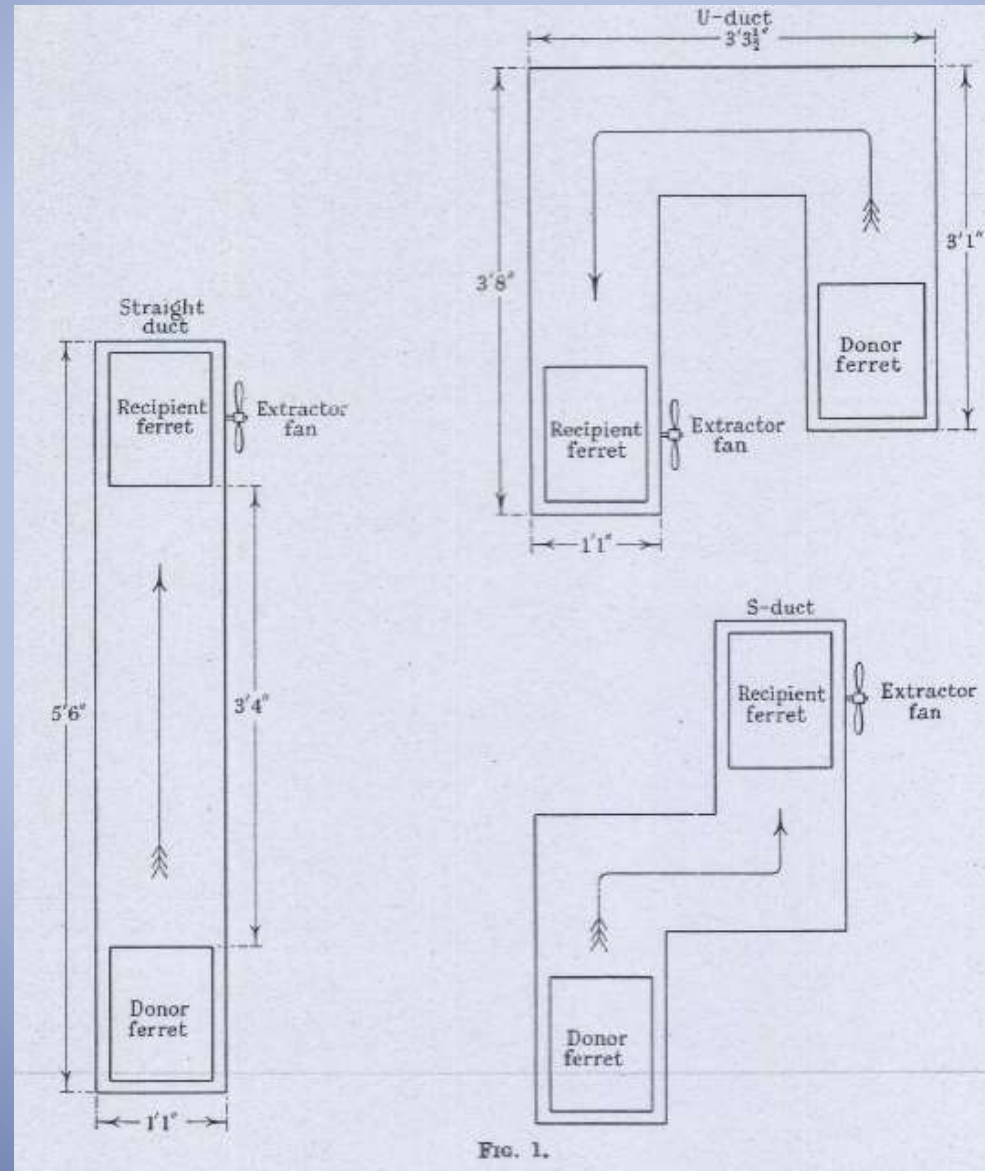
- Furets (souches humaines)
- Chevaux (souches équines)
- Cailles [HPAI A(H5N1)]
- Porcs [A(H1N1) pdm09]
- cobayes (souches humaines)

SPREAD OF INFECTION FROM THE RESPIRATORY TRACT OF THE FERRET. I. TRANSMISSION OF INFLUENZA A VIRUS.

C. H. ANDREWES AND R. E. GLOVER.

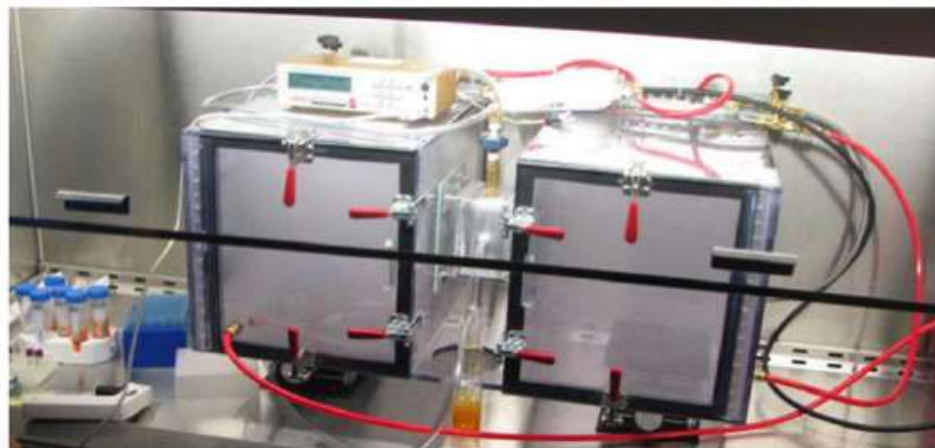
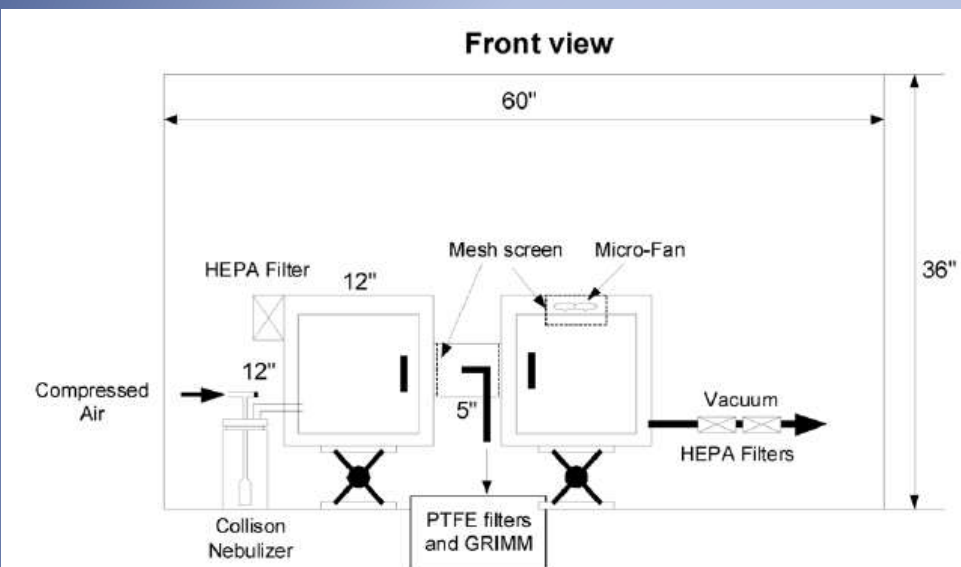
From the Farm Laboratories, National Institute for Medical Research, Mill Hill, London, N.W. 7.

Received for publication March 24, 1941.

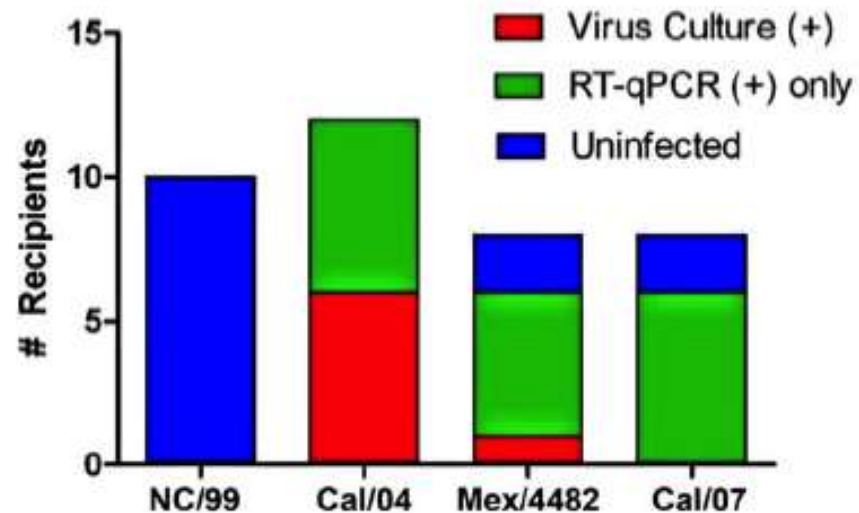


Exhaled Aerosol Transmission of Pandemic and Seasonal H1N1 Influenza Viruses in the Ferret

Citation: Koster F, Gouveia K, Zhou Y, Lowery K, Russell R, et al. (2012) Exhaled Aerosol Transmission of Pandemic and Seasonal H1N1 Influenza Viruses in the Ferret. PLoS ONE 7(4): e33118. doi:10.1371/journal.pone.0033118



Mode of diagnosis of infection following 3 h Aerosol Exposure

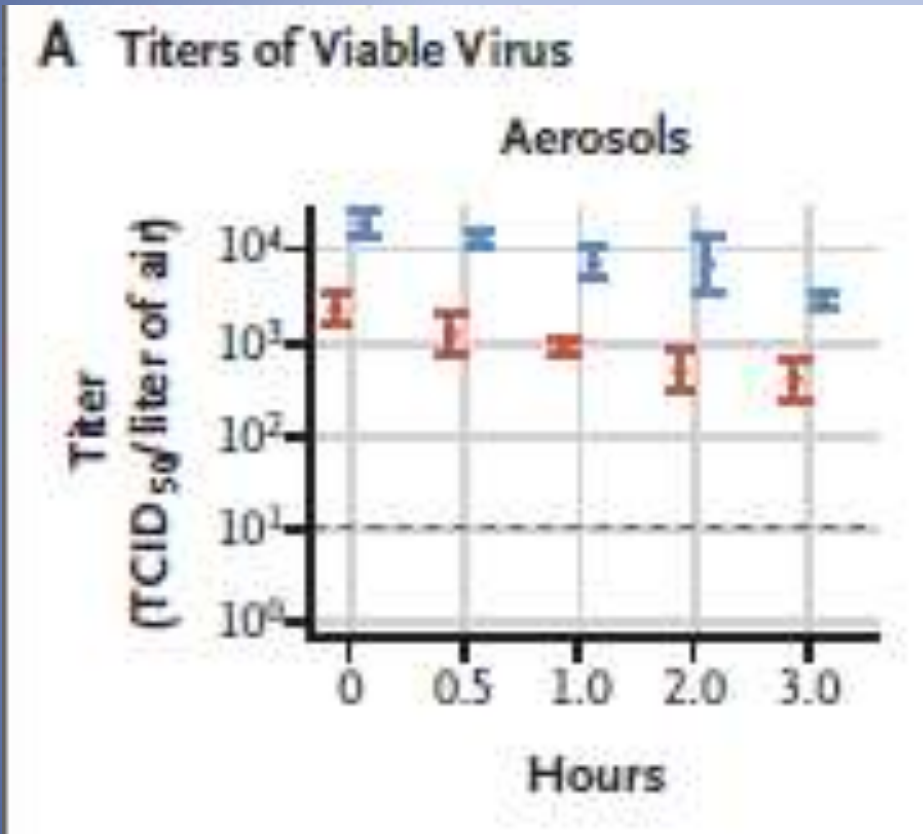


Citation: MacInnes H, Zhou Y, Gouveia K, Cromwell J, Lowery K, et al. (2011) Transmission of Aerosolized Seasonal H1N1 Influenza A to Ferrets. PLoS ONE 6(9): e24448. doi:10.1371/journal.pone.0024448

CORRESPONDENCE

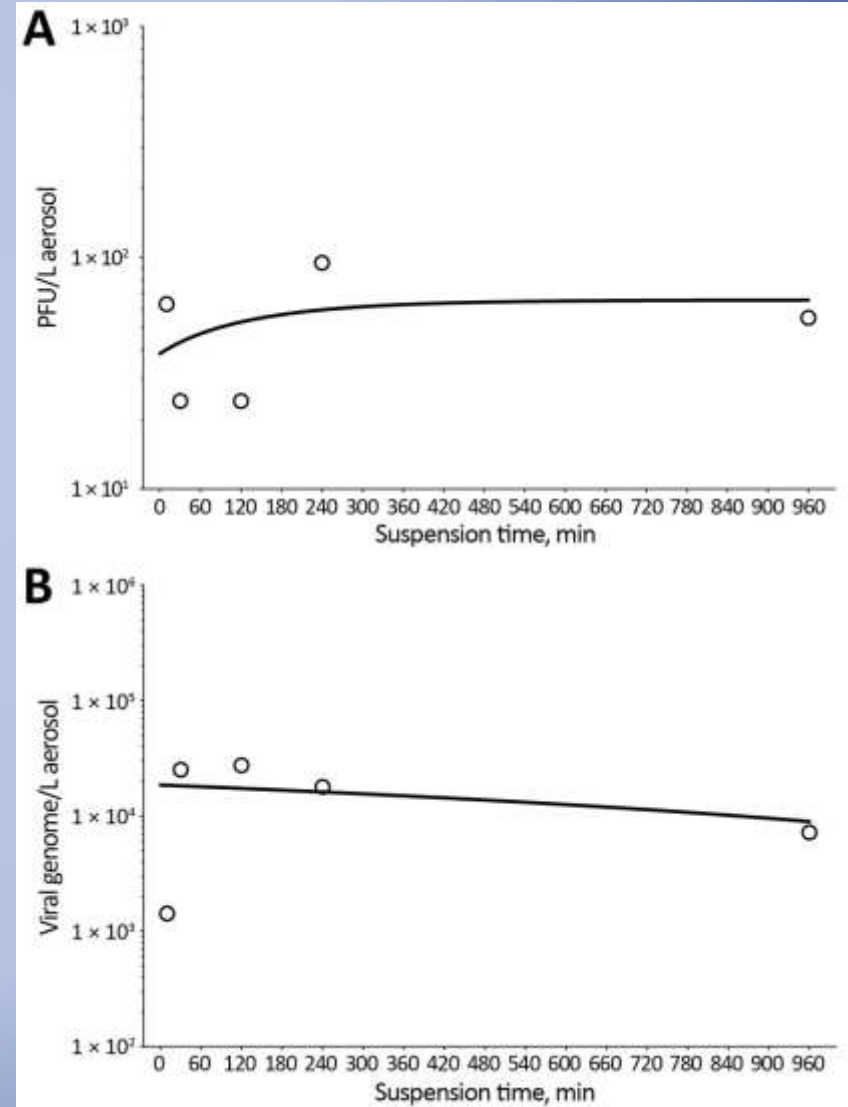
Aerosol and Surface Stability of SARS-CoV-2
as Compared with SARS-CoV-1

Van Doremalen et al

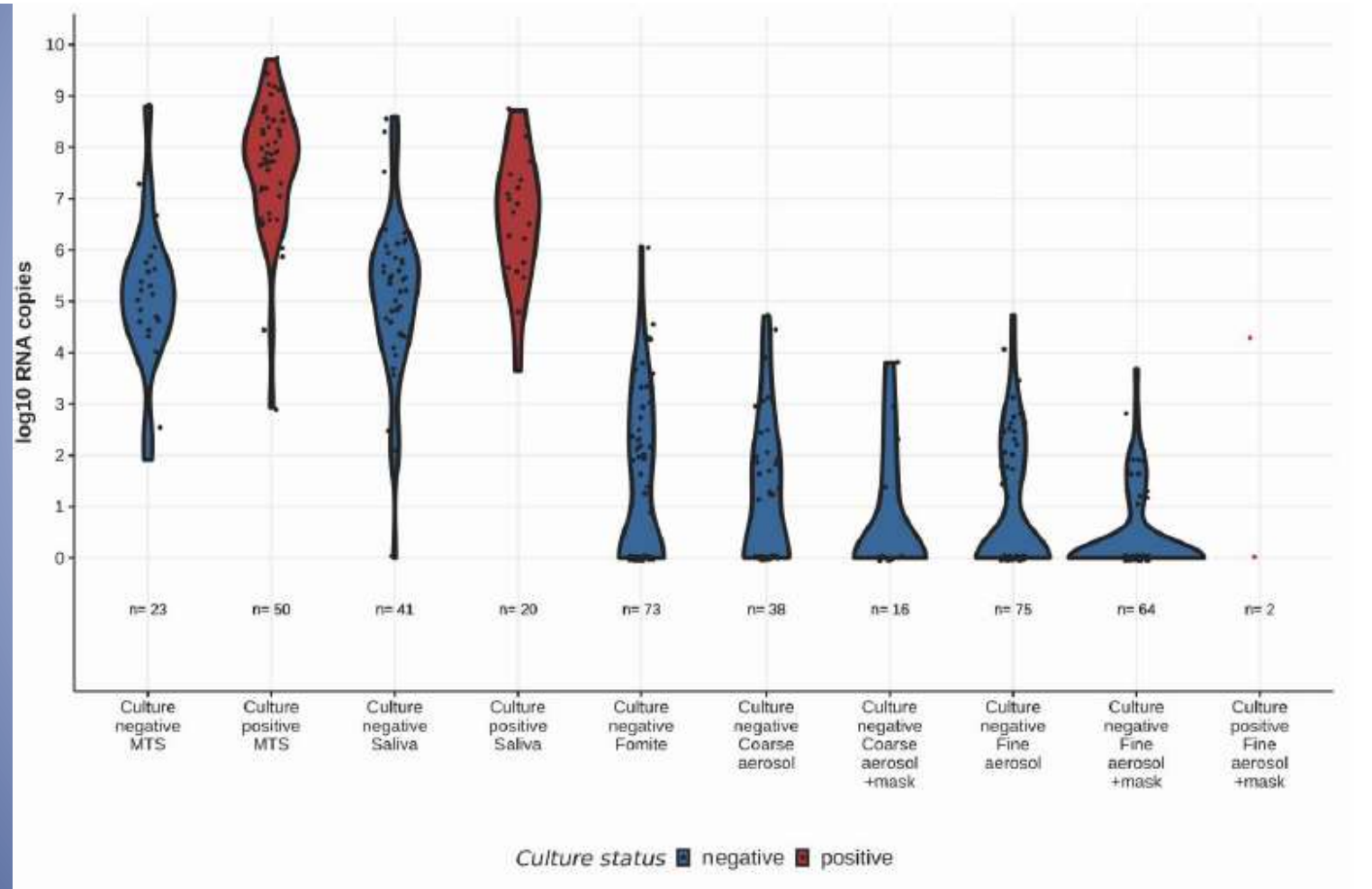


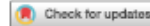
- SARS-CoV-2
- SARS-CoV-1

Volume 26, Number 9—September
2020 Dispatch
Persistence of Severe Acute
Respiratory Syndrome Coronavirus 2
in Aerosol Suspensions
Fears AC et al



Coarse (>5 μm) Aerosol	Alpha	4	4 (100)	2 (50)	6	6 (100)	3 (50)	140 (28, 730)	5.1×10^4
	Other	45	11 (24)	5 (11)	72	14 (19)	5 (7)	7 (3.2, 15)	2.6×10^4
Fine ($\leq 5 \mu\text{m}$) Aerosol	Alpha	4	4 (100)	3 (75)	6	6 (100)	4 (67)	580 (450, 740)	5.4×10^4
	Other	45	18 (40)	8 (18)	72	22 (31)	9 (12)	18 (9.1, 34)	2.8×10^3





OPEN

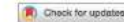
Aerosol and surface contamination of SARS-CoV-2 observed in quarantine and isolation care

Joshua L. Santarpia^{1,2,3}, Danielle N. Rivera², Vicki L. Herrera⁴, M. Jane Morwitzer⁴, Hannah M. Creager², George W. Santarpia², Kevin K. Crown², David M. Brett-Major⁴, Elizabeth R. Schnaubelt^{1,3}, M. Jana Broadhurst¹, James V. Lawler^{1,2}, St. Patrick Reid² & Jakob Levin^{1,2}

ARTICLE

<https://doi.org/10.1038/s41467-020-16670-2>

OPEN



Detection of air and surface contamination by SARS-CoV-2 in hospital rooms of infected patients

Po Ying Chia^{1,2,3,11}, Kristen Kelli Coleman^{4,11}, Yian Kim Tan^{5,11}, Sean Wei Xiang Ong^{1,2,11}, Marcus Gum⁵, Sok Kiang Lau⁵, Xiao Fang Lim⁵, Ai Sim Lim⁵, Stephanie Sutjipto^{1,2}, Pei Hua Lee^{1,2}, Than The Son⁴, Barnaby Edward Young^{1,2,3}, Donald K. Milton⁶, Gregory C. Gray^{4,7,8}, Stephan Schuster⁹, Timothy Barkham^{2,10}, Partha Pratim De^{2,3}, Shawn Vasoo^{1,2,3}, Monica Chan^{1,2}, Brenda Sze Peng Ang^{1,2,3,10}, Boon Huan Tan⁵, Yee-Sin Leo^{1,2,3,10}, Oon-Tek Ng^{1,2,3,12,13}, Michelle Su Yen Wong^{5,12}, Kalisvar Marimuthu^{1,2,10,12,13} & for the Singapore 2019 Novel Coronavirus Outbreak Research Team*

nature

<https://doi.org/10.1038/s41586-020-2271-3>

Accelerated Article Preview

Aerodynamic analysis of SARS-CoV-2 in two Wuhan hospitals

Received: 14 March 2020

Accepted: 20 April 2020

Accelerated Article Preview Published
online 27 April 2020

Yuan Liu, Zhi Ning, Yu Chen, Ming Guo, Yingjie Liu, Nirmal Kumar Gali, Li Shan, Yuesen Duan, Jing Cai, Dane Westerdahl, Xinjin Liu, Ke Xu, Kin-fai Ho, Haidong Kan, Qingyan Fu & Ke Lan

Centers for Disease
Control and Prevention

Volume 26, Number 7—July 2020

Dispatch

Aerosol and Surface Distribution of Severe Acute Respiratory Syndrome Coronavirus 2 in Hospital Wards, Wuhan, China, 2020

Zhen-Dong Guo¹, Zhong-Yi Wang¹, Shou-Feng Zhang¹, Xiao Li, Lin Li, Chao Li, Yan Cui, Rui-Bin Fu, Yun-Zhu Dong, Xiang-Yang Chi, Meng-Yao Zhang, Kun Liu, Cheng Cao, Bin Liu, Ke Zhang, Yu-Wei Gao, Bing Lu, and Wei Chen

Viable SARS-CoV-2 in the air of a hospital room with COVID-19 patients

John A. Lednicky, Michael Lauzardo, Z. Hugh Fan, Antarpreet Jutla, Trevor B. Tilly, Mayank Gangwar, Moiz Usmani, Sripriya Nannu Shankar, Karim Mohamed, Arantza Eiguren-Fernandez, Caroline J. Stephenson, Md. Mahbubul Alam, Maha A. Elbadry, Julia C. Loeb, Kuttinchantran Subramaniam, Thomas B. Waltzek, Kartikeya Cherabuddi, J. Glenn Morris Jr., Chang-Yu Wu



PII: S1201-9712(20)30739-6
DOI: <https://doi.org/10.1016/j.ijid.2020.09.025>

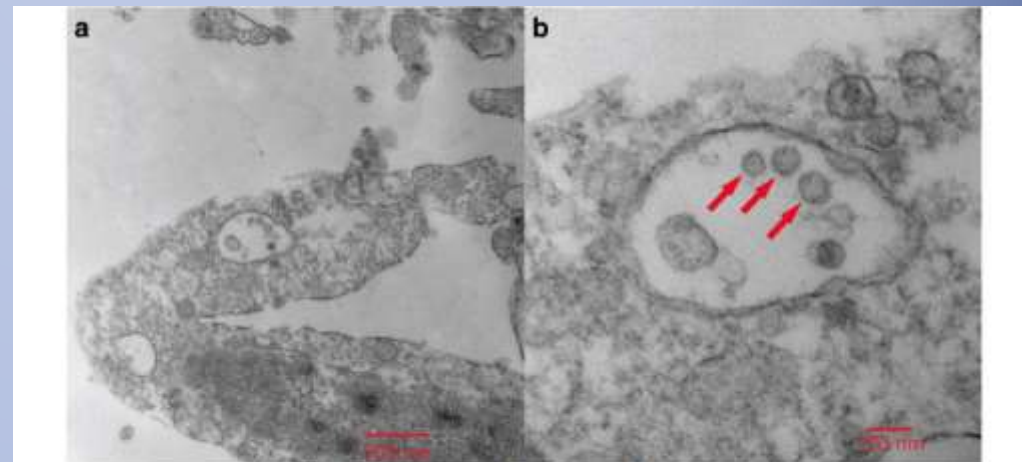
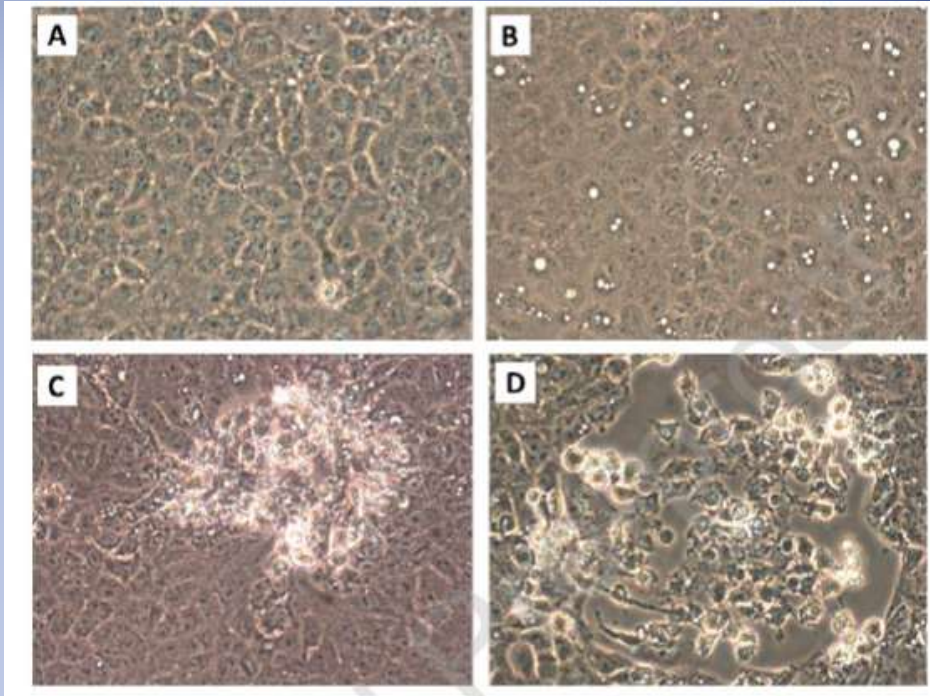


Fig. 3 Electron micrographs of SARS-CoV-2 virions cultivated from the sub-micron filter from Room 5C. The same image is shown at two magnifications: (A) $\times 30,000$ and (B) $\times 110,000$. Identifiable SARS-CoV-2 virions can be seen at both magnifications, and are indicated by red arrows in (B).

The size and culturability of patient-generated SARS-CoV-2 aerosol

Joshua L. Santarpia^{1,2,3,11,12}, Vicki L. Herrera^{1,4}, Danielle N. Rivera⁵, Shanna Ratriesar-Shumate^{1,2}, St. Patrick Reid^{1,6,11}, Daniel N. Ackerman⁷, Paul W. Denton⁸, Jacob W. S. Martens⁹, Ying Fang⁹, Nicholas Conran⁶, Michael V. Callahan⁷, James V. Lawler^{2,6}, David M. Brett-Major^{2,9} and John J. Lowe^{1,10,11}

Isolation of SARS-CoV-2 from the air in a car driven by a COVID patient with mild illness

John A. Lednicky,^{1,2} Michael Lauzardo,^{1,3} Md. M. Alam,^{1,2} Maha A. Elbadry,^{1,2} Caroline J. Stephenson,^{1,2} Julia C. Gibson,^{1,2} and J. Glenn Morris, Jr.^{1,3*}

ABSTRACT

We used a Sioutas personal cascade impactor sampler (PCIS) to screen for SARS-CoV-2 in a car driven by a COVID-19 patient. SARS-CoV-2 was detectable at all PCIS stages by PCR and was cultured from the section of the sampler collecting particles in the 0.25 to 0.50 μm size range.

Isolation of SARS-CoV-2 from the air in a car driven by a COVID patient with mild illness

John A. Lednicky^{a,b}, Michael Lauzardo^{a,c}, Md. M. Alam^{a,b}, Maha A. Elbadry^{a,b}, Caroline J. Stephenson^{a,b}, Julia C. Gibson^{a,b}, J. Glenn Morris Jr.^{a,c,*}

Submitted to *Indoor Air*

15 June 2020

Transmission of SARS-CoV-2 by inhalation of respiratory aerosol in the Skagit Valley Chorale superspreading event

Shelly L. Miller¹, William W Nazaroff², Jose L. Jimenez³, Atze Boerstra⁴, Giorgio Buonanno⁵, Stephanie J. Dancer⁶, Jarek Kurnitski⁷, Linsey C. Marr⁸, Lidia Morawska⁹, Catherine Noakes¹⁰

Centers for Disease Control and Prevention

MMWR

Morbidity and Mortality Weekly Report

Early Release / Vol. 69

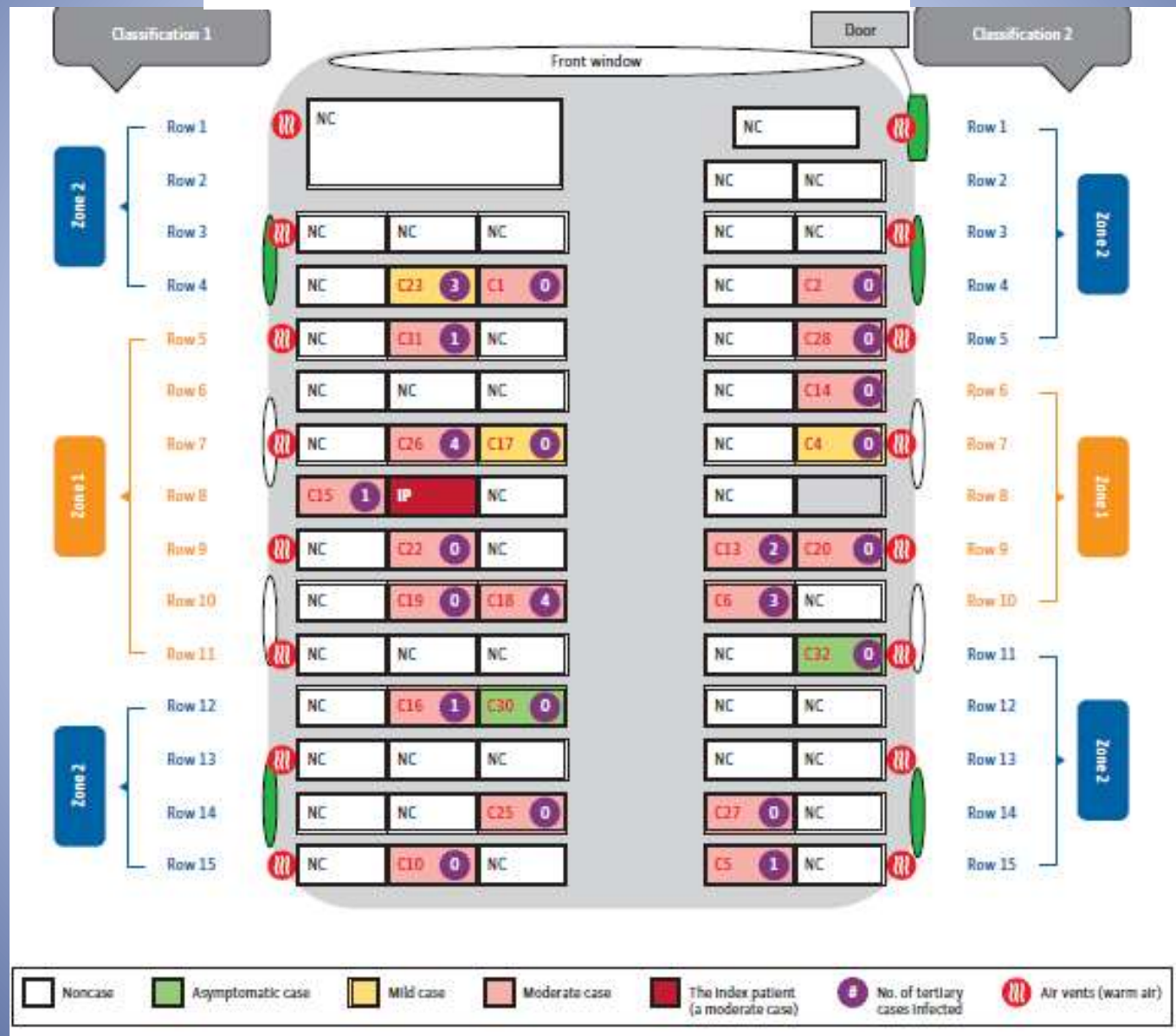
May 12, 2020

High SARS-CoV-2 Attack Rate Following Exposure at a Choir Practice — Skagit County, Washington, March 2020

Lea Hamner, MPH¹; Polly Dubbel, MPH¹; Ian Capron¹; Andy Ross, MPH¹; Amber Jordan, MPH¹; Jaxon Lee, MPH¹; Joanne Lynn¹; Amelia Ball¹; Simranjit Narwal, MSc¹; Sam Russell¹; Dale Patrick¹; Howard Leibrand, MD¹

Community Outbreak Investigation of SARS-CoV-2 Transmission Among Bus Riders in Eastern China

Ye Shen, PhD; Changwei Li, PhD; Hongjun Dong, MD; Zhen Wang, MD; Leonardo Martinez, PhD; Zhou Sun, MD; Andreas Handel, PhD; Zhiping Chen, MD; Enfu Chen, MD; Mark H. Ebell, MD, MS; Fan Wang, MA; Bo Yi, MD; Haibin Wang, MD; Xiaoxiao Wang, MD; Aihong Wang, MD; Bingbing Chen, MD; Yanling Qi, PhD; Lirong Liang, MD, PhD; Yang Li, PhD; Feng Ling, MD; Junfang Chen, MD; Guozhang Xu, MD



Evidence for probable aerosol transmission of SARS-CoV-2 in a poorly ventilated restaurant
Li Y et al

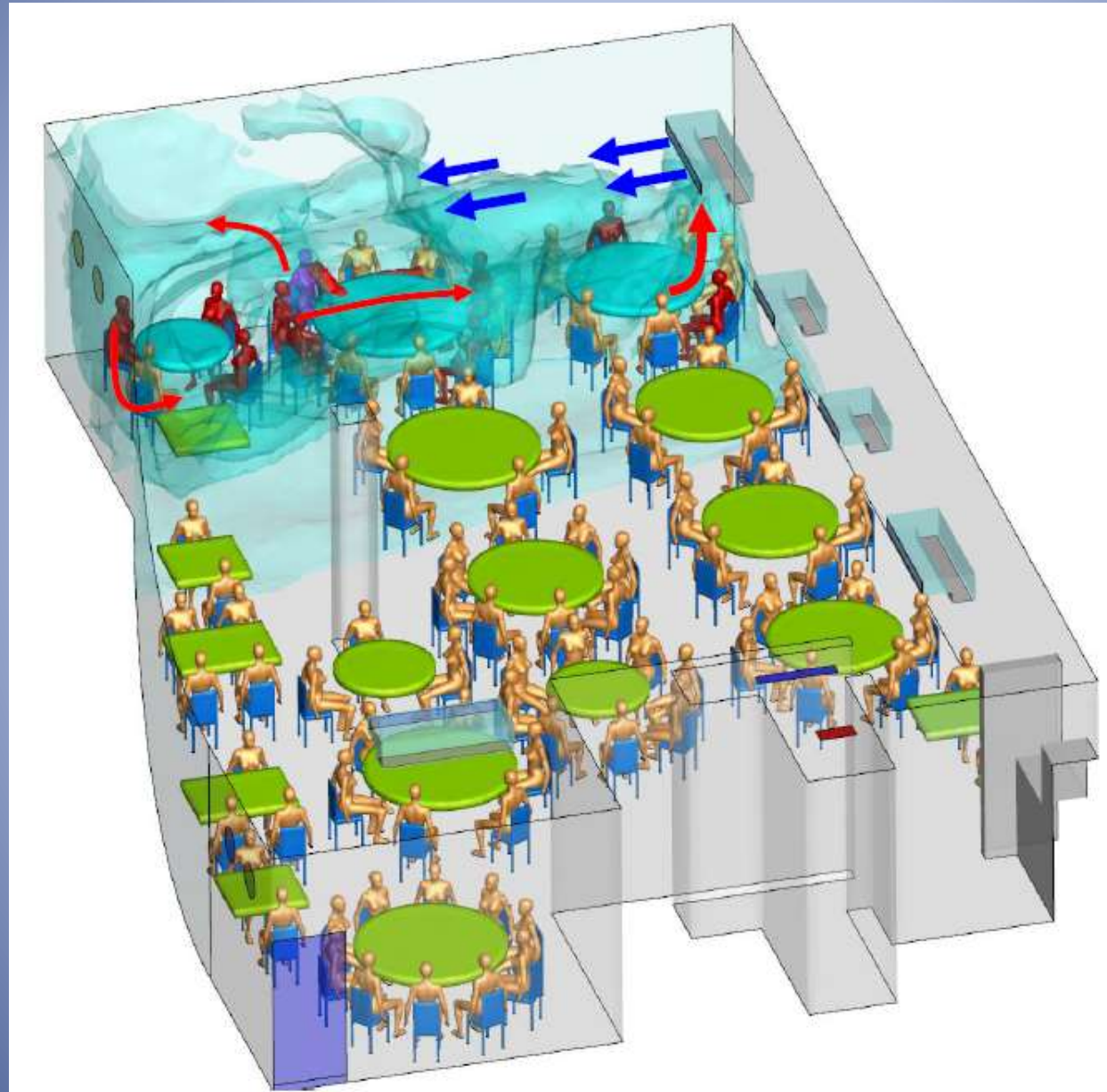


Figure 2

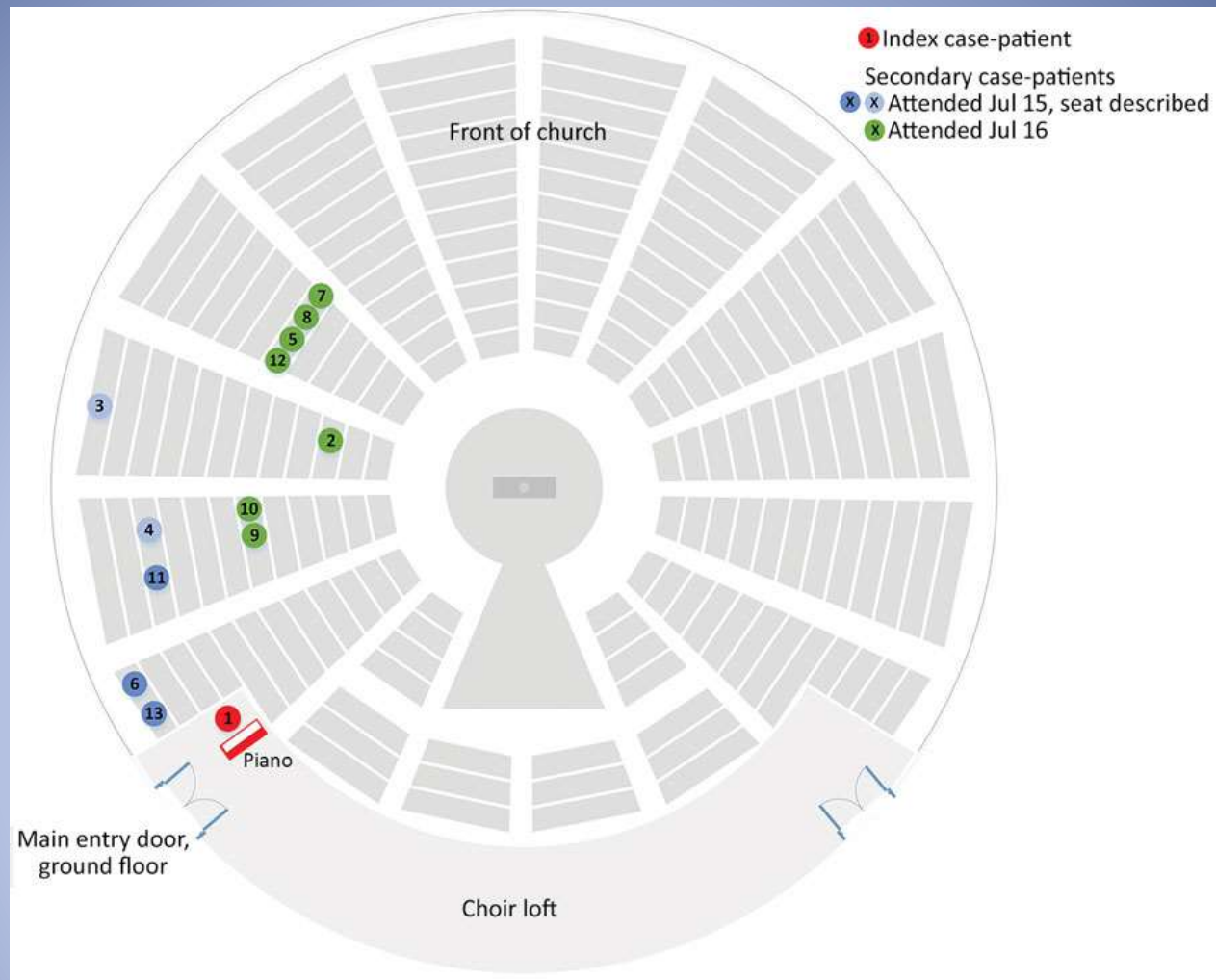



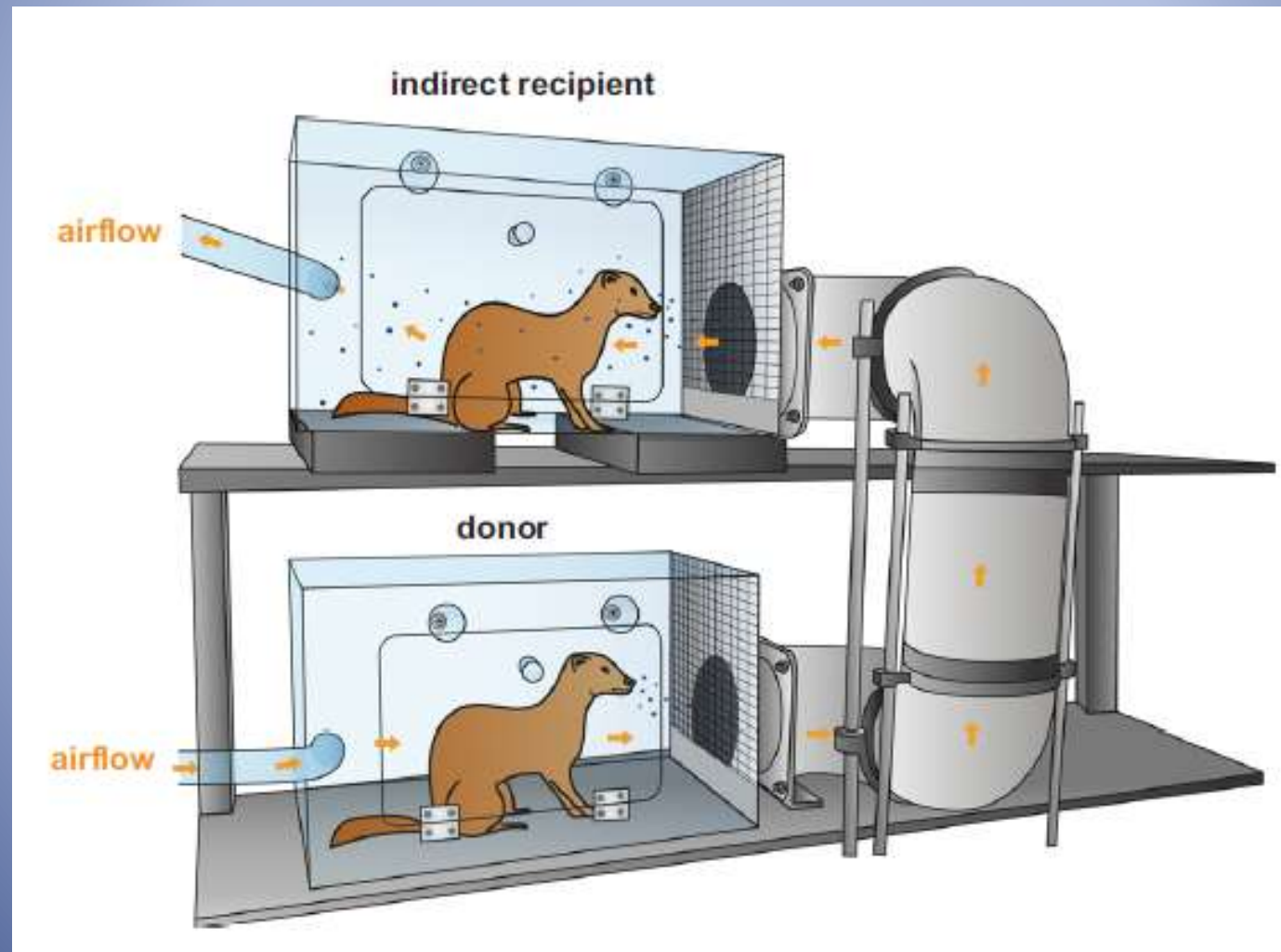


Figure 2. Schematic diagram of church layout showing seating locations of primary and secondary case-patients during an outbreak of infection with severe acute respiratory syndrome coronavirus 2, Australia, 2020. Case numbers are based on order of notification received by the Public Health Unit. Location of case-patients indicated in green and dark blue were confirmed on video recordings; the 2 case-patients indicated in light blue described their locations. The primary case-patient was located in an elevated loft ≈ 3 m above ground level. He was singing and playing the piano throughout the services and faced toward the piano. Other members of the congregation were seated throughout all sections of the church during the 4 services. Relatively more persons were seated in the front area of the church than in the sides or back.




SARS-CoV and SARS-CoV-2 are transmitted through the air between ferrets over more than one meter distance

Jasmin S. Kutter¹, Dennis de Meulder¹, Theo M. Bestebroer¹, Pascal Lexmond¹, Ard Mulders¹, Mathilde Richard ¹, Ron A. M. Fouchier ¹ & Sander Herfst ¹✉

NATURE COMMUNICATIONS | (2021)12:1653 | <https://doi.org/10.1038/s41467-021-21918-6> | www.nature.com/naturecommunications

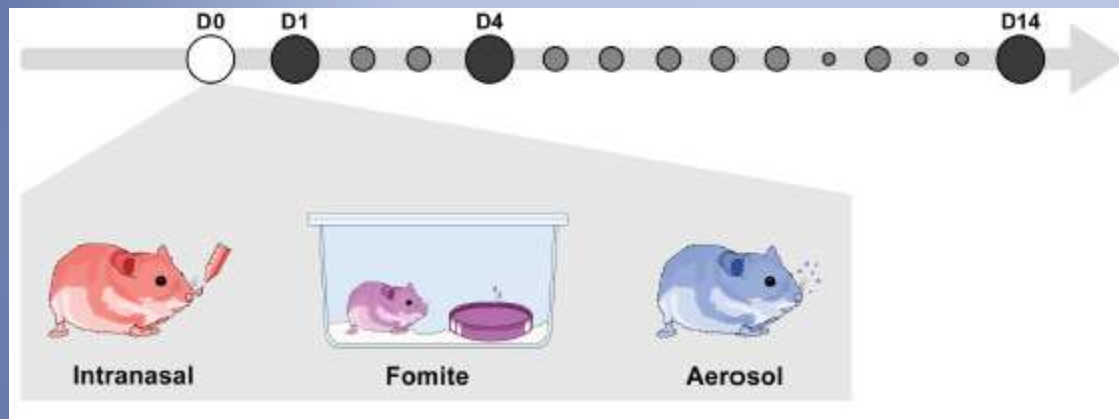


247 **Table 1. Virus transmission to recipient ferrets over various distances.**

Virus	Distance between donor and recipient	Recipient ferrets			
		Transmission	Onset shedding (dpe)	peak virus shedding (dpe)	peak virus titer (log ₁₀ TCID ₅₀ /ml)
A/H1N1 	10 cm ⁹	4 / 4	3, 3, 1, 3 [‡]	3, 3, 5, 5	4.8, 5.3, 4.5, 5.0
	> 1 m	4 / 4	5, 1, 3, - [‡]	7, 3, 3, -	5.3, 5.5, 6.0, -
SARS-CoV-2 	DC ⁶	4 / 4	3, 3, 1, 3 [†]	9, 7, 5, 7	3.5, 2.9, 2.3, 3.1
	10 cm ⁶	3 / 4	7, 3, 3 [†]	11, 9, 5	4.3, 3.0, 1.7
	> 1 m	2 / 4	1, 3 [†]	7, 5	1.6, 3.7
SARS-CoV 	DC ^{7§}	2 / 2	2, 2	8, 8	4.1 [¶]
	> 1 m	4 / 4	1, 1, 1, 3 [†]	5, 3, 5, 3	4.0, 3.6, 3.4, 2.6

SARS-CoV-2 disease severity and transmission efficiency is increased for airborne but not fomite exposure in Syrian hamsters.

Julia R. Port^{1*}, Claude Kwe Yinda^{1*}, Irene Offei Owusu¹, Myndi Holbrook¹, Robert Fischer¹, Trenton Bushmaker^{1,2}, Victoria A. Avanzato¹, Jonathan E. Schulz¹, Neeltje van Doremalen¹, Chad S. Clancy³, Vincent J. Munster^{1#}



pathology, higher virus loads and increased weight loss. Fomite exposure led to milder disease manifestation characterized by an anti-inflammatory immune state and delayed shedding pattern.”

“Despite a 10-fold lower inoculation dose, exposing Syrian hamsters to aerosolized SARS-CoV-2 326 resulted in more rapid virus replication in the lung and weight loss compared to I.N. inoculation.”

Aerosols of 1 -5 μm

Development of a coronavirus disease 2019 nonhuman primate model using airborne exposure

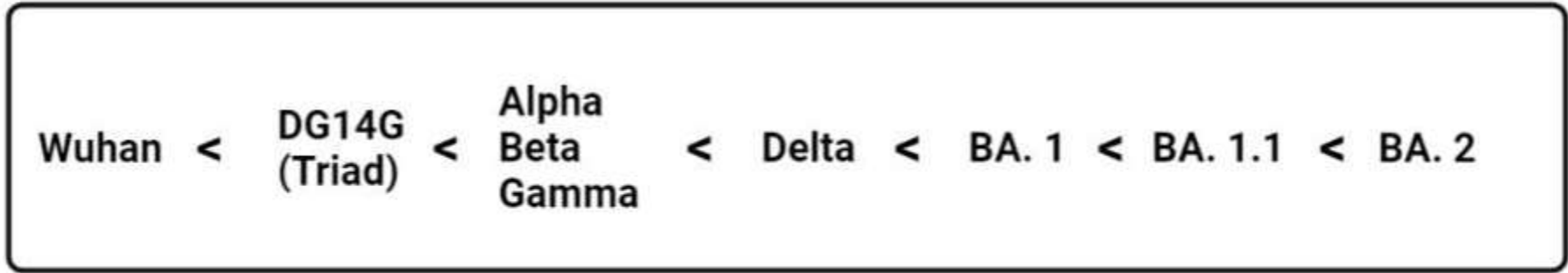
Sara C. Johnston^{1*}, Keersten M. Ricks², Alexandra Jay³, Jo Lynne Raymond⁴, Franco Rossi³, Xiankun Zeng⁴, Jennifer Scruggs⁴, David Dyer³, Ondraya Frick³, Jeffrey W. Koehler², Paul A. Kuehnert², Tamara L. Clements², Charles J. Shoemaker², Susan R. Coyne², Korey L. Delp², Joshua Moore³, Kerry Berrier³, Heather Esham³, Joshua Shamblin³, Willie Sifford³, Jimmy Fiallos³, Leslie Klosterman³, Stephen Stevens³, Lauren White³, Philip Bowling³, Terrence Garcia³, Christopher Jensen³, Jeanean Ghering³, David Nyakiti³, Stephanie Bellanca³, Brian Kearney⁵, Wendy Giles³, Nazira Alli³, Fabian Paz³, Kristen Akers⁵, Denise Danner⁵, James Barth⁵, Joshua A. Johnson⁵, Matthew Durant⁵, Ruth Kim⁵, Jay W. Hooper¹, Jeffrey M. Smith¹, Jeffrey R. Kugelman⁶, Brett F. Beitzel⁶, Kathleen M. Gibson⁵, Margaret L. M. Pitt⁷, Timothy D. Minogue², Aysegul Nalca^{8*}

PLOS ONE | <https://doi.org/10.1371/journal.pone.0246366> February 2, 2021

CMs have been investigated as a potential model for SARS-CoV-2, with variable disease findings noted following either IT/IN or IT/IN/ocular inoculation . Importantly, fever, which represents a prominent human disease sign and which was consistently noted for CM on the present study, was not noted for any CMs on these prior studies.

(1 -3 μm)

Transmission



Haseltine W.A. , Forbes Feb 23, 2022

